

# Department of Aerospace Engineering IIT Madras



**AS5213:** Design of MAVs and UAVs

**Group 5:** UAV Design Report

- **AE21B002 :** Abhigyan Roy
- **AE23M004 :** Vinu Mathew
- **AE23M008 :** Anish Konar
- **AE23M014 :** Gautham Anil
- **AE23M033 :** Satyam Chandra
- **AE23M006 :** Aditya Sai Deepak Rachagiri

# Contents

<b>1 Problem Definition</b>	<b>6</b>
1.1 Introduction . . . . .	6
1.1.1 Mission Statement . . . . .	6
1.1.2 Mission Motivation and Description . . . . .	6
1.1.3 Mission Profile . . . . .	7
1.2 Payload . . . . .	8
1.3 Data Collection . . . . .	10
<b>2 Weight and Power Estimation</b>	<b>15</b>
2.1 Data Collection . . . . .	15
2.2 Payload Weight . . . . .	16
2.3 Powerplant Selection . . . . .	16
2.4 First Weight Estimate . . . . .	18
<b>3 Thrust to Weight Ratios and Wing Loading</b>	<b>20</b>
3.1 Calculation of T/W Ratio . . . . .	20
3.2 Wing Loading . . . . .	24
3.2.1 Wing Loading for Takeoff . . . . .	24
3.2.2 Wing Loading for Climb Rate . . . . .	25
3.2.3 Wing Loading for Stall . . . . .	25
3.2.4 Wing Loading for Cruise . . . . .	25
3.2.5 Wing Loading for Absolute Ceiling . . . . .	26
3.2.6 Wing Loading for Loiter . . . . .	26
3.2.7 Wing Loading Selection . . . . .	27
3.2.8 Power Loading vs Wing Loading Plot . . . . .	27
<b>4 Second Weight Estimate</b>	<b>28</b>
<b>5 Wing Design</b>	<b>29</b>
5.1 Design Lift Coefficient Calculations . . . . .	29
5.1.1 Cruise . . . . .	29
5.1.2 Stall . . . . .	29
5.1.3 Take-Off . . . . .	30
5.1.4 Climb . . . . .	30
5.2 Airfoil Selection . . . . .	30
5.3 Angle of Incidence . . . . .	34
5.4 Taper Ratio . . . . .	34
5.5 Sweep Angle . . . . .	37
5.6 Wing Configuration . . . . .	37
5.7 Dihedral Angle . . . . .	39
5.8 Aileron . . . . .	39
<b>6 Fuselage Design</b>	<b>40</b>
6.1 Fuselage Length . . . . .	40
6.2 Fuselage Sizing . . . . .	41

<b>7 Tail Design</b>	<b>43</b>
7.1 Tail Configuration . . . . .	43
7.2 Optimum Tail Arm . . . . .	45
7.3 Horizontal Tail . . . . .	45
7.4 Vertical Tail . . . . .	47
<b>8 Landing Gear Design</b>	<b>48</b>
8.1 Landing gear Configuration . . . . .	48
8.2 Landing Gear retraction . . . . .	49
8.3 Landing Gear Geometry . . . . .	49
8.3.1 Position of Main LG and Nose LG . . . . .	49
8.3.2 Landing Gear Track . . . . .	50
8.3.3 Landing Gear Height . . . . .	50
8.3.4 Landing Gear Overturn Angle . . . . .	51
8.4 Load on each Landing Gear . . . . .	52
8.5 Selection of Tyres . . . . .	52
8.6 Nose Wheel Steering System . . . . .	52
<b>9 Three View Diagram</b>	<b>53</b>
9.1 CAD Model of UAV . . . . .	53
9.2 Centre of Gravity . . . . .	54
<b>10 Stability Analysis</b>	<b>56</b>
10.1 Simulation Analysis . . . . .	56
10.1.1 Modelling the UAV . . . . .	56
10.1.2 Simulation Results . . . . .	58
10.2 Neutral point . . . . .	59
10.3 Longitudinal Static Stability . . . . .	59
10.3.1 Pitching Moment Coefficient . . . . .	60
10.3.2 Static Margin . . . . .	60
10.4 Directional Static Stability . . . . .	60
10.5 Lateral Stability . . . . .	61
10.6 Control Surfaces . . . . .	62
10.6.1 Aileron . . . . .	62
10.6.2 Elevator . . . . .	62
10.6.3 Rudder . . . . .	63
10.7 Flight Controller . . . . .	63
<b>11 Performance Calculation</b>	<b>64</b>
11.1 Drag Polar . . . . .	64
11.1.1 $S_{wet}$ . . . . .	64
11.1.2 $C_{D_0}$ Calculation . . . . .	64
11.2 Final Power Estimates . . . . .	65
11.2.1 Takeoff . . . . .	65
11.2.2 Climb . . . . .	66
11.2.3 Cruise . . . . .	66
11.3 Range and Endurance . . . . .	66
11.4 V - n Diagram . . . . .	66
<b>12 Final Summary</b>	<b>68</b>
<b>13 Appendix</b>	<b>71</b>
13.1 First Weight and Power Estimate Calculation . . . . .	71
13.2 T/W Calculation . . . . .	74
13.3 W/S Calculation for Multiple Phases of Flight . . . . .	76
13.4 Second Weight Estimate Calculation . . . . .	78
13.5 Fuselage Length Estimation . . . . .	80
13.6 Conceptual Horizontal Tail Area Sizing Calculation . . . . .	81
13.7 Drag Polar Calculation . . . . .	82

# List of Figures

1.1.1 Area of Coverage . . . . .	7
1.1.2 Mission Profile . . . . .	8
1.2.1 Workswell Wiris Pro . . . . .	8
1.2.2 Prana Air SQUAIR . . . . .	9
1.3.1 The Blue Shark F250 . . . . .	10
1.3.2 The E-384 UAV . . . . .	11
1.3.3 The Bayraktar Mini . . . . .	11
1.3.4 The Raven B RQ-11 . . . . .	12
1.3.5 Albatross . . . . .	13
1.3.6 JOUAV CW15 . . . . .	13
1.3.7 JOUAV CW 007 . . . . .	14
2.1.1 Weight Estimate Data . . . . .	16
2.3.1 Tattu LiPo Battery [17] . . . . .	18
2.4.1 First Weight Estimate . . . . .	19
3.1.1 $(L/D)_{max}$ vs $v_{cruise}$ . . . . .	22
3.1.2 $(L/D)_{max}$ vs $\sqrt{AR}_{wet}$ . . . . .	22
3.1.3 T16 Propellers . . . . .	23
3.1.4 T Motor . . . . .	23
3.1.5 T-MOTOR AT7215 Datasheet . . . . .	23
4.0.1 Second Weight Estimate . . . . .	28
5.2.1 Plot of chosen Airfoil GOE 553 . . . . .	31
5.2.2 Airfoil Lift vs Angle of Attack and Drag Polar . . . . .	32
5.2.3 Airfoil Moment vs Angle of Attack and Airfoil Lift-To-Drag vs Lift Coefficient . . . . .	32
5.2.4 3D image of rectangular wing for chosen airfoil . . . . .	32
5.2.5 Wing Lift vs Angle of Attack and Wing Drag Polar . . . . .	33
5.2.6 Wing Lift-To-Drag vs Angle of Attack . . . . .	33
5.2.7 Wing with Flap . . . . .	33
5.2.8 Wing Lift vs Angle of Attack with and without flaps . . . . .	34
5.4.1 Different taper ratios for a wing and their $C_L$ variation [29] . . . . .	35
5.4.2 Tapered Wing with taper ratio 0.6 . . . . .	35
5.4.3 Drag Polar of wing with and without taper . . . . .	36
5.4.4 Air Stream over Rectangular Wing . . . . .	36
5.4.5 Air Stream over Tapered Wing . . . . .	36
6.1.1 Fuselage Length Estimation . . . . .	40
6.2.1 Components Arrangement in Fuselage . . . . .	41
7.3.1 $C_M$ vs $\alpha$ for Wing . . . . .	45
7.3.2 Total $C_M$ vs $\alpha$ for Varying $V_H$ and Tail Area ( $S_t$ ) . . . . .	46
7.3.3 Airfoil for Tail: Symmetric Airfoil NACA0014 . . . . .	46
7.4.1 Airfoil of Vertical Tail . . . . .	47
8.0.1 Landing Gear Parameters [28] . . . . .	48

8.1.1 Tricycle Landing Gear . . . . .	49
8.2.1 Comparison of Fixed vs Retractable system . . . . .	49
8.3.1 Landing Gear Design . . . . .	50
8.3.2 Take off Ground Clearance . . . . .	51
8.3.3 Clearance Angle Estimation . . . . .	51
8.3.4 Estimation of Overturn Angle . . . . .	51
8.4.1 Loads acting on the LG . . . . .	52
 9.1.1 Isometric View . . . . .	53
9.1.2 Front View . . . . .	53
9.1.3 Top View . . . . .	54
9.1.4 Components . . . . .	54
9.2.1 CG . . . . .	54
9.2.2 CG without Wing . . . . .	55
 10.1. <b>I</b> XFLR5 UAV Model Isometric View . . . . .	57
10.1. <b>II</b> XFLR5 UAV Model Front View . . . . .	57
10.1. <b>III</b> XFLR5 UAV Side View with sizings . . . . .	58
10.1. <b>IV</b> UAV Lift $C_L$ and Moment $C_M$ vs Angle of Attack $\alpha$ . . . . .	58
10.1. <b>V</b> UAV Directional Stability $C_n$ and Roll Stability $C_l$ vs Sideslip angle $\beta$ . . . . .	58
10.1. <b>VI</b> UAV $C_M$ vs $C_L$ and $C_L/C_D$ vs Angle of Attack $\alpha$ . . . . .	59
10.6.1(a) Top view of the wing and aileron for reference ; (b) Side view of the wing and aileron for reference[28] . . . . .	62
 11.1. <b>I</b> Drag Polar . . . . .	65
11.4. <b>IV</b> - n diagram . . . . .	67

# List of Tables

1.3.1 Blue Shark F250 Specifications . . . . .	10
1.3.2 E-384 UAV Specifications . . . . .	11
1.3.3 Bayraktar Mini UAV Specifications . . . . .	12
1.3.4 Raven B RQ-11 Specifications . . . . .	12
1.3.5 Albatross Specifications . . . . .	13
1.3.6 JOUAV CW-15 Specifications . . . . .	14
1.3.7 JOUAV CW 007 Specifications . . . . .	14
2.1.1 Reference UAV Weight Data . . . . .	15
2.2.1 Payload Weight Data . . . . .	16
2.3.1 Approximate values used to estimate Power required for different Flight Phases . . . . .	17
2.3.2 Battery Specifications . . . . .	18
3.1.1 Cruise Condition . . . . .	21
3.2.1 Parameters for Wing Loading Calculation . . . . .	24
3.2.2 Wing Loading at different Flight Conditions . . . . .	27
5.2.1 Airfoil Data . . . . .	30
5.2.2 Geometric and Aerodynamic Characteristics GOE 553 . . . . .	31
6.1.1 Fuselage Lengths for different UAVs . . . . .	40
6.2.1 Fuselage Dimensions . . . . .	42
10.3.1 Longitudinal Stability Parameters . . . . .	60
11.1.1 Area of components (m <sup>2</sup> ) . . . . .	64
12.0.1 General UAV Specifications . . . . .	68
12.0.2 Wing Specifications . . . . .	68
12.0.3 Horizontal Tail Specifications . . . . .	69
12.0.4 Vertical Tail Specifications . . . . .	69
12.0.5 Fuselage Specifications . . . . .	69
12.0.6 Weights . . . . .	69
12.0.7 Aerodynamic Characteristics . . . . .	70

# Chapter 1

## Problem Definition

### 1.1 Introduction

#### 1.1.1 Mission Statement

Monitoring of Flora and Fauna and the environment of forests in the Chennai AOR and Mapping of Forest Cover which includes security based Surveillance of the forest within the said Area of Responsibility.

#### 1.1.2 Mission Motivation and Description

Forests are indispensable in the fight against climate change, serving as crucial carbon sinks that absorb significant amounts of carbon dioxide from the atmosphere. Through the process of photosynthesis, trees and vegetation capture CO<sub>2</sub>, storing it in their biomass and releasing oxygen back into the air. Moreover, forests help regulate regional and global climates by influencing atmospheric moisture levels and reflecting sunlight through their canopy cover. Deforestation, however, disrupts this balance, releasing stored carbon and reducing the Earth's capacity to mitigate greenhouse gas emissions. Preserving and restoring forests not only safeguards biodiversity but also mitigates climate change impacts, making them essential components of sustainable environmental stewardship.

For an efficient management of the Forest cover within the city, it is crucial to monitor the highly dynamic and ever-changing nature of forests which requires timely data acquisition. The process for which is often time, labor and cost-intensive and requires data coverage across a large spatial region. Medium-range medium-endurance UAVs have thus been identified as a cost-effective readily available alternative. Short-term and quick surveys at scheduled time intervals of the forest cover can aid in achieving quantifiable results that can help assess the real-time Environmental state of the forest.

With the mission motivation defined, the group has decided to list its mission description as below.

1. To design a UAV with sufficient range and endurance to be able to fly within the Chennai City Limits to monitor the forest cover of the city. The UAV should have to have an initial cruise altitude of about 80m to be able to provide an aerial survey of the Chennai AOR. Post which, the UAV would fly into the specific target area at a lower altitude of about 40m to be able to provide the user detail inputs of the Target forest area.
2. The UAV should be equipped with sufficient sensors to be able to undertake environment monitoring and surveillance. The UAV should enable the user to be able to monitor the forest by indicating different stressors that attribute to the overall health of the forest. The environmental parameters such as temperature, relative humidity, and presence of harmful gases in the air will produce quantifiable results for the health monitoring. The UAV could also be utilized for monitoring and tracking of specific Fauna in the forest and to monitor the state of the water bodies in the forest or within the city limits.
3. The UAV has the potent capability of carrying out high range aerial survey within a very short period of time and hence can be used for early detection of forest fires. This should enable the user to activate fire services well in time for efficient management of the forest fire.

4. As the UAV is an airborne platform equipped with an optical sensor, it could also be used for assessment of damage from environmental calamities such as floods, cyclones, earthquakes, etc. where a ground survey assessment would not be a feasible solution.
5. The UAV should be equipped with optical and Infrared sensors. This could also be used for active and passive surveillance missions to reduce trespassing and illegal timber poaching activities. With the aid of the IR sensors, the UAV would be able to capture the presence and movement of the intruders even under the forest canopy.

### 1.1.3 Mission Profile

Based on the aforementioned Mission objectives, the Mission Profile is generated below.

#### Phase I:

##### **Take Off and Climb:**

The UAV should have a very low startup time and hence be readily deployed on short notice to achieve the desired objective. Also, it would need to have a low take-off distance and a high Rate of Climb is desirable to be able to reach cruising altitude as soon as possible.

#### Phase II:

##### **Cursory Data Acquisition:**

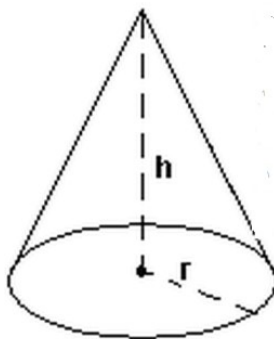


Figure 1.1.1: Area of Coverage

Based on the area of coverage of the Chennai City limits and considering the height of the tallest tree within the city limits to be about 40m, Two cruising altitudes of 80 meters and 40 meters have been identified for the UAV operation. In the Cursory data acquisition phase with an altitude of 80m, the area of coverage comes upto about  $6943 \text{ m}^2$ . This would be sufficient for a cursory scan of the target area. The UAV is expected to be able to loiter for about 20–30 minutes at an altitude of about 80m. This would enable us to carry out a high range aerial survey to collect higher spatial data and identify areas of interest.

#### Phase III:

##### **Detail Data Acquisition:**

Post completion of the Cursory Data Acquisition phase, the UAV would be employed to loiter at a lower cruise altitude of about 40 m for about 45–60 minutes to monitor the environment of the forest at tree top levels. The area of coverage at an altitude of 40m would be about  $3471 \text{ m}^2$ . This cruise altitude will also provide detailed information of the target AOR at a higher resolution. This would enable the user to extract detailed source information for a better assessment of the data acquired.

## Phase IV:

### Descent and Landing:

The UAV must then carry out a descent at nominal descent angles, maintaining correct approach speeds, to carry out a safe landing at the desired landing strip.

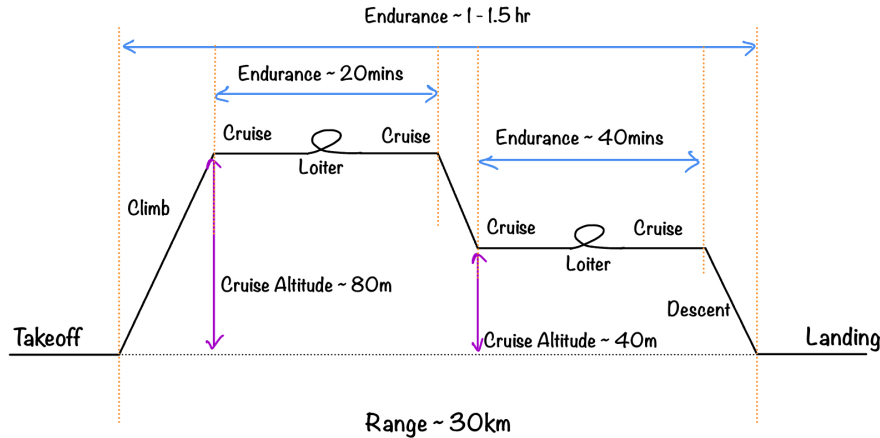


Figure 1.1.2: Mission Profile

## 1.2 Payload

To effectively achieve the mission objectives outlined previously, it is imperative that the UAV be outfitted with appropriate avionics equipment. The following payloads have been carefully chosen to ensure the successful attainment of the mission objectives.

### 1) Thermo – Optical sensor : Workswell Wiris Pro



Figure 1.2.1: Workswell Wiris Pro

The Workswell WIRIS Pro is a thermodiagnostic device. Its thermal camera is equipped with an LWIR microbolometric sensor with  $640 \times 512$  px resolution (in the 7.5 – 13.5 m range), and its 'Super Resolution Mode' functionality can deliver a final thermogram in  $1266 \times 1010$  px resolution. The RGB camera comes with Full HD ( $1920 \times 1080$  px) resolution and provides an absolutely unrivaled optical ultrazoom 10x in real-time (6.9° to 58.2° field of vision). The highest possible temperature that the thermal camera can measure is 1,500 °C. The thermo optic sensor is equipped with an advanced operating system for thermal cameras, ensuring full real-time data streaming and control during flights, with easy camera control through various interfaces. Also an interface used for integrating UAV cameras with MAVLINK systems, allowing for advanced control and data transmission capabilities.

Thermal Camera Specification	
IR Camera Resolution	640 x 512 pixels
IR Super Resolution Mode	1 266 x 1 010 pixels
FPA active sensor size	1.088 x 0.8705 cm
Temperature ranges	-25 °C to +150 °C -40 °C to +550 °C optional temperature range +50 – 1 000 °C optional temperature range +400 – 1 500 °C
Temperature sensitivity	Standard 0.05 °C (50 mK) or optional 0.03 °C (30 mK)
Accuracy	±2 % or ±2 °C (in temperature range -10 °C to +150°C and 0 °C to +550°C, after stabilization, climate chamber and black body testing for all products)
Frame rate	30 Hz or 9 Hz
Spectral range / detector	7.5 – 13.5 m / Uncooled VOx microbolometer

Digital Visual Camera	
Resolution	1 920 x 1 080 pixels (Full HD), 1/3" sensor. Auto white balance, Wide dynamic range, Backlight compensation, Exposure and Gamma control
Optical zoom	10x optical zoom with vibration compensation.
View angle	ultra zoom 6.9° - extra wide 58.2°, focal 33.0 mm - 3.3 mm
Noise reduction	Special 3D noise reduction function
Focus	Autofocus with Direct Focus Zoom synchronization

## 2) AIR QUALITY SENSOR – PRANA AIR SQUAIR

SQUAIR monitor is a air quality monitoring device that can detect particulate matters and gas parameters. It detects PM10, PM2.5, CO, CO2, O3, NO2, SO2, TVOC, HCHO, noise, light, temperature & humidity.



Figure 1.2.2: Prana Air SQUAIR

Instrument Specification	
Features	Description
Weight	227 g
Power Supply	5 V DC
Connectivity	Wi-Fi/GSM/RS485
Storage	Micro-SD card/Cloud storage

### SENSOR SPECIFICATIONS

Parameters	Sensor Type	Range	Resolution	Accuracy
Temperature	Digital Sensor	-30 to 60 °C	0.1 °C	±0.1°C
Relative Humidity	Digital Sensor	0 to 99%	1%	+/- 1 % RH
PM 10, PM 2.5 &PM 1	Light Scattering	1 to 1999	1 µg/m³	0-150 µg/m³

### 1.3 Data Collection

To enable a better understanding of the physical attributes of the UAV required to achieve the aforementioned Mission Profile, data has been collected about the various other UAVs available with similar mission profiles. The same is as listed below:-

#### 1. Blue Shark F250



Figure 1.3.1: The Blue Shark F250

GENERAL CHARACTERISTICS	PERFORMANCE
Capacity: 220 W	Cruise speed: 20-27 m/s
Length: 126 cm	Range: up to 150 km
Wingspan: 250 cm	Endurance: 4 hrs without Payload, 3.2 hrs with 1.2 Kg payload
Gross Weight: 13.5 kg	
Power plant: 2*65 27000 mAH HED Li-ion	
ADDITIONAL FEATURES	
Pitot Tube	
CG balance	
Aileron Servo	
Tail Quick Release	
High quality motors and props	
Tail ECS ventilation	
Laser Radar	
ViewPro Gimbal Camera	
Surveying and Mapping Camera	

Table 1.3.1: Blue Shark F250 Specifications

## 2. UAV E384



Figure 1.3.2: The E-384 UAV

GENERAL CHARACTERISTICS	PERFORMANCE
Max Payload: 1.7 Kg	Cruise speed: 12-20 m/s
Length: 130 cm	Range: 70 km
Wingspan: 190 cm	Endurance: 90 mins Flight time
Gross Weight: 2.5 Kg	Maximum Altitude: 3960 m
ADDITIONAL FEATURES	
Handshot Take-off	
Belly landing	
Equipped with Sony R10C Camera plus companion computer	
Quanum i8 2.4GHz Transmitter Radio with 8 channels	

Table 1.3.2: E-384 UAV Specifications

## 3. Bayraktar Mini UAV



Figure 1.3.3: The Bayraktar Mini

GENERAL CHARACTERISTICS	PERFORMANCE
Length: 1.2 m	Cruise speed: 55 - 75 kmph
Wingspan: 2 m	Endurance: 100-120 min
Gross Weight: 4.5 kg	Operational Altitude: 600 m
Dimensions: 17 x 35 x 43 cm	Maximum Altitude: 1200 m
Powerplant: Brushless Electric Motor	
Fuel Capacity: 2 Low Current Chargers, 1 High Current Charger, 1 Transformer, 220V AC, 12V DC	
Input Possibility	
ADDITIONAL FEATURES	
Handshot Take-Off & Automatic Parachute Landing	
Joystick Assisted Semi-Automatic Flight	
Stall Speed Control Capability &	
Reliable Digital Communication System with 15 km range	
Automatic Return to Home and	
Automatic Landing in Case of Communication Loss	
Interchangeable 2 Axis Day/Night Cameras	

Table 1.3.3: Bayraktar Mini UAV Specifications

#### 4. Raven B RQ-11



Figure 1.3.4: The Raven B RQ-11

GENERAL CHARACTERISTICS	PERFORMANCE
Length: 0.9 m	Cruise speed: 32 kmph
Wingspan: 1.4 m	Dash speed: 81 kmph
Gross Weight: 2.2 kg	Endurance: 75+ min
Powerplant: Single Aveox 27/26/7-AV Electric motor	Range: 10 km
	Operational Altitude: 30-152 m
	Maximum Altitude: 4267 m
ADDITIONAL FEATURES	
Handshot Take-Off	
Autonomous or manual precision deep-stall landing	
10 km link range, Equipped with 2 ISR Cameras Mantis i23	
Real Time Video and Infrared Imagery	

Table 1.3.4: Raven B RQ-11 Specifications

## 5. Albatross



Figure 1.3.5: Albatross

General Characteristics	Performance
<b>Wingspan:</b> 300 cm	<b>Cruise speed:</b> 68 km/hr
<b>Fuselage:</b> 740 mm x 200 mm x 150 mm	<b>Range:</b> Up to 250 km
<b>MTOW:</b> 10 kg	<b>Endurance:</b> Up to 4hrs flight time
<b>Powerplant:</b> Electric Motors with Custom Li ion batteries	
Additional Features	
Multiple cameras are fitted for capturing reliable aerial imagery to suit every mapping job.	
This drone seamlessly integrates with the user-friendly PX4 software, allowing you to plan missions, monitor progress, and analyze results directly from your base station.	
It can resist winds up to 32 km/hr.	
It is made of carbon fiber and fiberglass composite.	

Table 1.3.5: Albatross Specifications

## 6. JOUAV CW-15



Figure 1.3.6: JOUAV CW15

General Characteristics	Flight Performance
<b>MTOW:</b> 16.5 Kg	<b>Endurance:</b> 180 min
<b>Fuselage:</b> 2.06 m	<b>Cruising Speed:</b> 61 km/h
<b>Wingspan:</b> 3.54 m	<b>Wind Resistance:</b> 10.8-13.8 m/s
<b>Powerplant:</b> Electrical Motor (Low noise, brushless)	<b>Ceiling:</b> 6500 m
<b>Payload:</b> 3 kg	<b>Max Takeoff Altitude:</b> 4500 m
<b>Takeoff Landing:</b> VTOL	
<b>Additional features</b>	
The CW-15 can carry various payloads. Therefore, it can be applied to a wide range of tasks, including mapping, surveillance, public safety, oil and gas pipeline inspection, etc.	
Automatically avoid obstacles in flight, detect other drones equipped with ADS-B modules, adapt to more terrain, and avoid dangerous landing points such as roofs and cliffs.	
Fly in high altitude, high humidity, low-temperature, and light rain conditions with self-heating airspeed tube and battery.	
It can also easily fly in complex electromagnetic environments.	

Table 1.3.6: JOUAV CW-15 Specifications

## 7. JOUAV CW-007



Figure 1.3.7: JOUAV CW 007

General Characteristics	Flight Performance
<b>MTOW:</b> 6.8 kg	<b>Endurance:</b> 55 min
<b>Fuselage:</b> 1.3 m	<b>Cruising Speed:</b> 61.2 km/h
<b>Wingspan:</b> 2.2 m	<b>Wind Resistance:</b> 10.8-13.8 m/s
<b>Propulsion:</b> Electrical Motor (Low noise, brush less)	<b>Ceiling:</b> 6000 m
<b>Payload:</b> 1 kg	<b>Max Takeoff Altitude:</b> 4500 m
<b>Additional Features</b>	
Modular design: Takes less than 2 minutes for setup or take down.	
High Efficiency: Single flight can finish 4 km <sup>2</sup> of 1:500 scale, 6 km <sup>2</sup> of 1:1000 scale, 12 km <sup>2</sup> of 1:2000 scale.	
Dual GPS and Dual compass, it can smoothly switch to the backup unit if there is a fault.	
Ground-based and handheld control station setup.	

Table 1.3.7: JOUAV CW 007 Specifications

## Chapter 2

# Weight and Power Estimation

### 2.1 Data Collection

To obtain an estimate of the weight a historical data collection was carried out. The data has been obtained by survey of UAVs with similar mission profiles. Table 2.1.1 below shows a compilation of the weight data collected of currently flying Radio Controlled (RC) electrically powered model airplanes.

S. No.	UAV	Take-Off Weight Estimate ( $W_o$ ) (kg)	Empty Weight Ratio ( $W_{empty}/W_o$ ) (kg)	Battery Weight (kg)
1.	Blue Shark F250	13.5	0.43	4.6
2.	JOUAV CW 007	6.8	0.55	2.5
3.	JOUAV CW 015	16.5	0.54	4.6
4.	Albatross: Long Range Drone	10	0.44	1.2 per battery
5.	Blue Shark F320	24	0.34	4*2.57
6.	Skywalker X5 Pro	2.5	0.84	0.488

Table 2.1.1: Reference UAV Weight Data

*Note:- For the case of Albatross where number of batteries was not available, it has been assumed to be 2.*

*Also, since exact weights were not available in open source, the weights have been calculated based on the type of battery and their capacity.*

Using the above data collected, we can fit a curve through it which would be our design curve for weight estimation. The equation of the curve fit which compares the empty weight fraction with the total flying weight would follow:

$$\frac{W_{empty}}{W_o} = AW_o^L \quad (2.1.1)$$

[19] where A and L are constant, and L is less than 0. Using similar UAV data, we used linear regression to find that **A = 1.0744** and **L = -0.2695**.

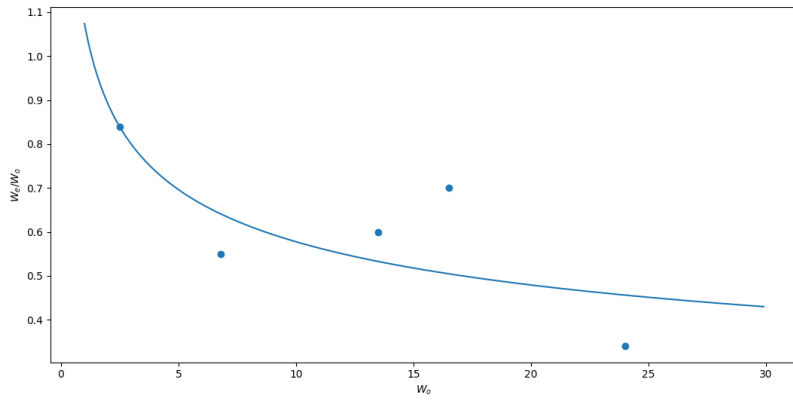


Figure 2.1.1: Weight Estimate Data

## 2.2 Payload Weight

For the successful completion of the mission objective of Environmental Monitoring and Mapping of Forest Cover including Security based Surveillance, we would require a optical sensor, thermal sensor and a weather based sensor. Additionally, the sensors need to be placed on a stabilized platform with suitable gimbals. Based on a brief market survey we finalised the below mentioned components for the completion of the mission objective. We also kept a 0.5kg buffer for any other extra accessories.

Sl No	Payload	Payload Weight (kg)
1	Integrated Thermal and Optical Sensor - Workswell WIRIS	0.68
2	Weather Sensor - Prana air SQUAIR	0.25
3	Gimbal for optical stabilization	0.4
4	Misc (connectors + wires + supports)	0.17
Total Payload Weight		1.5

Table 2.2.1: Payload Weight Data

**Design Payload Weight = 1.5 kg**

**Max Payload Weight = 2.0 kg**

## 2.3 Powerplant Selection

Now, we estimate the power consumption in different phases of flight and hence, can choose an appropriate battery for the UAV.

The power required during cruise is calculated using the following equation.

$$P_{cruise} = T_{cruise}v_{cruise} = \frac{1}{2}\rho v_{cruise}^3 SC_D \quad (2.3.1)$$

[19] where,  $v_{cruise} = 18$  m/s,

$$T_{cruise} = D = \frac{1}{2}\rho v_{cruise}^2 SC_D \text{ and}$$

$$\text{drag coefficient for cruise, } C_D = C_{D_0} + \frac{1}{\pi e AR} \left( \frac{W}{\frac{1}{2}\rho v_{cruise}^2 S} \right)^2$$

The power required during climb is calculated using the following equation.

$$P_{climb} = T_{climb}v_{climb} = \frac{1}{2}\rho v_{climb}^3 SC_D + Wv_{climb}\sin\gamma \quad (2.3.2)$$

[28] where,  $v_{climb} = \frac{2}{\sin 10^\circ} = 11.51 \text{ m/s}$

$T_{climb} = D + W \sin \gamma = \frac{1}{2} \rho v_{climb}^2 S C_D + W \sin \gamma$ ,  $\gamma$  being the climb angle, and drag coefficient for climb,  $C_D = C_{D_o} + \frac{1}{\pi e A R} \left( \frac{W \cos \gamma}{\frac{1}{2} \rho v_{climb}^2 S} \right)^2$

The power required during takeoff is calculated using the following equation.

$$P_{takeoff} = \frac{1}{2} \rho v_{takeoff}^3 C_{D_{takeoff}} \quad (2.3.3)$$

[28] where,  $v_{takeoff} = 1.2 v_{stall}$  and

drag coefficient for climb,  $C_{D_{takeoff}} = C_{D_o} + \phi \frac{1}{\pi e A R} \left( \frac{W}{\frac{1}{2} \rho v_{climb}^2 S} \right)^2$ , with the ground effect,  $\phi = \frac{(16h/b)^2}{1+(16h/b)^2}$

$$v_{stall} = \sqrt{\frac{2W}{\rho C_{L_{max}} S}} \quad (2.3.4)$$

[28]

Using the above equations, and substituting values from a design profile of a similar UAV as cited in [18], the following assumptions have been referenced.

Sl. No.	Parameters	Values
1	Aspect Ratio	8.89
2	$C_{D_o}$	0.03
3	$C_{L_{max}}$	0.82
4	Wing Planform Area	0.76

Table 2.3.1: Approximate values used to estimate Power required for different Flight Phases

Using the above data and the equations above, we get

	$Power_{phase}$	$T_{phase}$
$P_{takeoff}$	129.3016 W	10 s
$P_{climb}$	284.1195 W	5 min
$P_{cruise}$	128.9291 W	1 hour

Total Watt Hour =  $\sum P_{phase} T_{phase} = 152.9650$  Watt Hour

$$mAh = \frac{Wh * 1000}{Voltage} \quad (2.3.5)$$

Thus, estimated battery capacity for 9V DC Supply = **16996.11 mAh**

Additionally, we would also require battery power to run the payload sensors. We have approximated that the power requirement for all the sensors to work throughout the duration of flight and reached a final battery capacity estimate.

Hence, the total battery capacity required for the UAV can be approximated to **18000 mAh**.

Based on the requirements of the mission profile and weight considerations, we have taken the battery type to be a Li-Po Battery, for which the Specific Energy is about 100 Watthr/kg.



Figure 2.3.1: Tattu LiPo Battery [17]

Table 2.3.2: Battery Specifications

Specification	Value
Minimum Capacity	18000mAh
Configuration	6S1P / 22.2V / 6Cell
Discharge Rate	15C
Max Burst Discharge Rate	30C
Net Weight ( $\pm 20g$ )	2270g
Dimensions	205.5mm Length x 94.2mm Width x 79.5mm Height
Discharge Plug	XT90 plug
Charge Plug	XT90

We get the weight of the battery to be about 2.270 Kg. Which we round off to 2.3 kg for positive tolerance.

## 2.4 First Weight Estimate

We split the total weight of the aircraft into the sum of the empty weight (airframe), the battery weight, and the payload weight because the aircraft under design is an unmanned aerial vehicle with electric propulsion as shown in the equation below.

$$W_o = W_{empty} + W_{battery} + W_{payload} \quad (2.4.1)$$

[28] The weight estimation was done with a Python Script. 13.1 The weight estimation process estimates our Final Total weight  $W_o$  and our Empty Weight Fraction. It starts with fixing the Payload Weight = 2.3 kg, Battery Weight = 2 kg and initially guessing weight fraction = 0.5. We then estimate  $W_o$  from the equation given below,

$$W_o = \frac{W_{payload} + W_{battery}}{1 - \frac{W_{empty}}{W_o}} \quad (2.4.2)$$

[28] Which initially gives a value of  $W_o = 8.0$  kg. After that we substitute the estimated  $W_o$  into the design curve equation that we fit previously and get an estimated Empty Weight Fraction

$$\frac{W_{empty}}{W_o} = 1.206 * W_o^{-0.3} \quad (2.4.3)$$

[28] Using this new Empty Weight Fraction, we again use Equation 2.4 to estimate  $W_o$ . This process is iterated a few more times, and converges at around iteration number 9 where we get a final estimate of Total Weight  $W_o = 9.61$  kg and an **Empty Weight Fraction of 0.58**.

Given below is the Plot for Total Weight Estimate vs No. of Iterations.

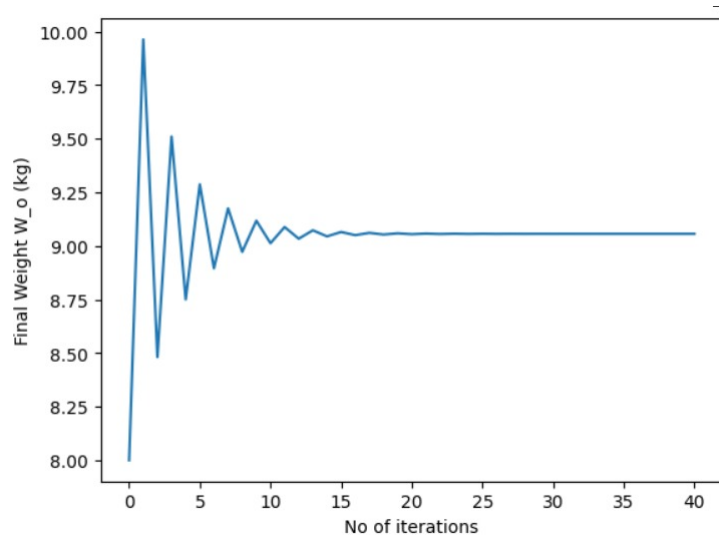


Figure 2.4.1: First Weight Estimate

## Chapter 3

# Thrust to Weight Ratios and Wing Loading

### 3.1 Calculation of T/W Ratio

The lift ( $L$ ) generated by an aircraft is given by:

$$L = \frac{1}{2}\rho V^2 S C_L \quad (3.1.1)$$

[28] The drag ( $D$ ) experienced by the aircraft is given by:

$$D = \frac{1}{2}\rho V^2 S C_D \quad (3.1.2)$$

[28] The lift-to-drag ratio ( $L/D$ ) is then:

$$\frac{L}{D} = \frac{C_L}{C_D} \quad (3.1.3)$$

[28] where  $C_D$  is given as,

$$C_D = C_{D_o} + \left( \frac{1}{\pi e A R} \right) C_L^2 \quad (3.1.4)$$

[28] To find the maximum ( $L/D$ ), we differentiate ( $L/D$ ) with respect to the  $C_L$  and set it to zero to get the maxima.  $\frac{d(L/D)}{dC_L} = 0$ . We substitute the value back in equation 3.11 to get the following result.

$$\left( \frac{L}{D} \right)_{max} = \sqrt{\frac{\pi e A R}{4 C_{D_o}}} \quad (3.1.5)$$

[28] For cruise, the thrust-to-weight ratio is equal to  $(\frac{L}{D})_{max}$

$$\left( \frac{T}{W} \right)_{cruise} = \frac{1}{(\frac{L}{D})_{max}} = \sqrt{\frac{4 C_{D_o}}{\pi e A R}} \quad (3.1.6)$$

[28] The formula for the zero-lift drag coefficient ( $C_{D_0}$ ) is given by: [25]

$$C_{D_o} = \frac{C_f \cdot S_{wet}}{S_{ref}} \quad (3.1.7)$$

[28] where,

$C_f$  is the skin friction coefficient, which depends on factors such as the surface roughness, Reynolds number, and flow conditions

$S_{wet}$  is the wetted area of the aircraft, representing the total surface area exposed to airflow

$S_{ref}$  is the reference area, which is usually the wing area for aircraft

The skin friction coefficient  $C_f$  can be estimated using the Von-Karman relation which is a good approximation for flow over a variety of slope. We are making this assumption as we have a blended wing configuration.

$$C_f = \frac{0.074}{Re^{1/7}} \quad (3.1.8)$$

[28] where,

$C_f$  is the skin friction coefficient

$Re$  is the Reynolds number based on the length of the object.

The Reynolds number  $Re$  is defined as:

$$Re = \frac{\rho \cdot V \cdot c}{\mu} \quad (3.1.9)$$

[28] where,

$\rho$  is the density of the fluid (air). We take an average value for the altitude we operate.

$V$  is the velocity of the flow, which we take the cruise velocity of the UAV.

$c$  is a characteristic length of the object, in this case the chord length

$\mu$  is the dynamic viscosity of the fluid

The Oswald Efficiency Factor, denoted by  $e$ , is a dimensionless parameter used in aerodynamics to describe the efficiency of an aircraft's wings in producing lift.

$$e = \frac{1}{1.05 + 0.007 \cdot \pi AR} \quad (3.1.10)$$

[28] where,

$e$  is the Oswald Efficiency Factor.[25]

$AR$  is the aspect ratio of the wings.

Based on the above equations and the open source information, the following table has been tabulated.

Sl. No.	UAV	$C_{D_o}$	$(L/D)_{max}$	$(T/W)_{min}$	Aspect Ratio	$V_{cruise}$ (m/s)
1	Green Raven	-	19.05	0.05249344	5.55	30
2	ITU Tailless UAV	-	26	0.03846154	.89	20
3	Sitaria	-	20.6875	0.04833837	4	16
4	Slybird Mini UAV	-	14	0.07142857	6	16
5	JOUAV CW-007	1.04654517e-04	13.37336828	0.07477548	3.27	16.67
6	JOUAV CW-015	9.67597940e-05	13.9069789	0.07190634	8.89	20
7	BlueShark F250	0.02275	17.30398653	0.05779	11.255	20

Table 3.1.1: Cruise Condition

We plot  $(L/D)_{max}$  vs  $v_{cruise}$  and  $(L/D)_{max}$  vs  $\sqrt{AR}$  from this data and find the regression curve for each curve. 13.2

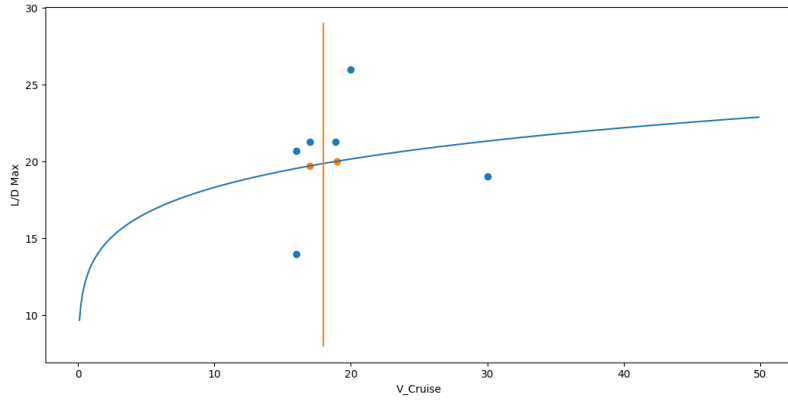


Figure 3.1.1:  $(L/D)_{max}$  vs  $v_{cruise}$

We obtain the  $(L/D)_{max}$  value of 19.4824 for  $v_{cruise} = 18$  m/s matching our mission profile and use it to find the appropriate aspect ratio ( $AR = 8.3$ ) in the next graph. From this value of AR,  $e = 0.81$ .

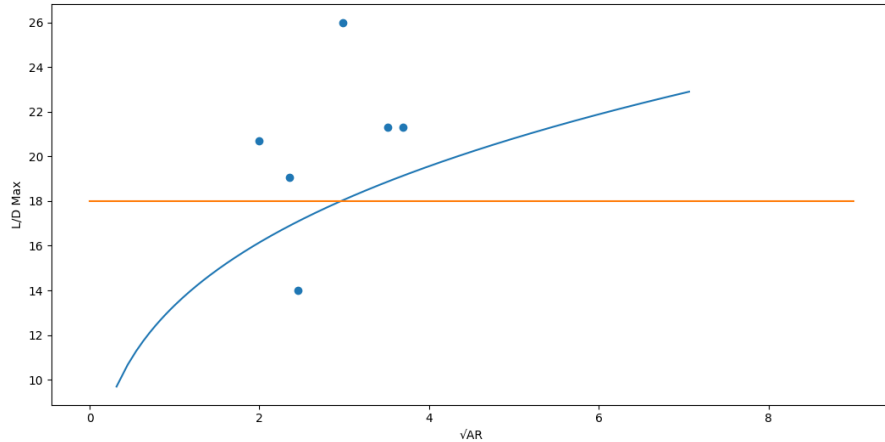


Figure 3.1.2:  $(L/D)_{max}$  vs  $\sqrt{AR_{wet}}$

Using the power equations

$$P_{takeoff} = \left( \frac{T}{W} \right)_{min} W v_{takeoff} \quad (3.1.11)$$

[28]

$$P_{climb} = \left( \frac{T}{W} \right)_{min} L_{max} v_{climb} + W v_{climb} \sin \gamma \quad (3.1.12)$$

[28]

$$P_{cruise} = \left( \frac{T}{W} \right)_{min} W v_{cruise} \quad (3.1.13)$$

[28] and the T/W graph,  $P_{takeoff} = 105.79$  Watt,  $P_{cruise} = 100.90$  Watt,  $P_{climb} = 1880.27$  Watt. Based on this power estimation and the first weight estimate, we have decided to use the AT7215 T-Motor[26] along with TF16\*8[27] propeller.



Figure 3.1.3: T16 Propellers



Figure 3.1.4: T Motor

The datasheet of the motor chosen has a range of power values that encompasses our requirements.

Test Report											
Type	Propeller	Throttle	Voltage (V)	Current (A)	Power (W)	RPM	Torque (N·m)	Thrust (g)	Efficiency (g/W)	Operating Temperature (°C)	
19*10	AT7215	40%	44.25	5.64	249.81	3494	0.532	1833	7.34		
		45%	44.22	7.41	327.75	3890	0.650	2312	7.05		
		50%	44.15	10.26	453.08	4356	0.795	2878	6.35		
		55%	44.08	13.28	585.57	4813	0.946	3477	5.94		
		60%	44.02	16.59	730.16	5206	1.110	4086	5.60		
		65%	43.91	21.80	957.40	5698	1.337	4903	5.12	/	
		70%	43.79	27.16	1189.47	6128	1.562	5710	4.80		
		75%	43.66	33.60	1466.85	6547	1.821	6582	4.49		
		80%	43.53	39.60	1723.40	6882	2.050	7366	4.27		
		90%	43.23	53.83	2327.01	7599	2.537	8911	3.83		
		100%	42.84	71.55	3065.09	8208	3.126	10555	3.44		

Figure 3.1.5: T-MOTOR AT7215 Datasheet

## 3.2 Wing Loading

For a better estimate of the wing loading for our Mini UAV, it has been calculated at various phases of flight. The flight profile relevant towards deciding a reasonable Wing Loading has thus been divided into the following.

1. Take off
2. Climb
2. Cruise
4. Absolute ceiling
5. Loiter

Based on the data collected for various Mini UAVs having similar profiles, the following parameters have been assumed for the purpose of calculation of the wing loading at various phases of flight.

Sl. No.	Parameter	Value
1	$C_{D_o}$	0.04
2	$C_L/C_{D_{max}}$	19.48
3	$C_{L_{max}}$	1.56
4	AR	8.3
5	e	0.81
6	$V_{Stall}$	10 m/s
7	$V_{Cruise}$	18 m/s
8	Rate of Climb	2 m/s
9	Angle of Climb	12°

Table 3.2.1: Parameters for Wing Loading Calculation

### 3.2.1 Wing Loading for Takeoff

For the estimation of Wing loading during the take off segment, two approaches have been utilised. Namely, a graphical estimation based on the equation stated below [28] and approximate estimate for a quantitative numerical assessment.

$$\left(\frac{W}{P}\right)_{S_{TO}} = \frac{1 \exp(0.6gC_{D,G}S_{TO}\frac{1}{W/S})}{-\left(+\frac{C_{D,G}}{C_{L,R}}\right)\left[\exp\left(0.6gC_{D,G}S_{TO}\frac{1}{W/S}\right)\right]} \frac{P}{V_{TO}} \quad (3.2.1)$$

[28] Substituting the below mentioned values gives us the following.

$$= 1.225 \text{ kg/m}^3, g = 9.81 \text{ m/sec}, S_{TO} = 10\text{m}, \mu = 0.03 \text{ (Dry concrete/ Asphalt)}$$

$$\begin{aligned} C_{D,G} &= C_{D,TO}C_{L,TO} \\ C_{D,TO} &= C_{D_{o,TO}} + KC_{L,TO}^2 \\ C_{D_{o,TO}} &= C_{D_o} + C_{D_{o,LG}} + C_{D_{o,HLD_{TO}}} \end{aligned}$$

Typical values of  $C_{D_o}$ ,  $C_{D_{o,LG}}$  and  $C_{D_{o,HLD_{TO}}}$  are 0.03, 0.009, 0.005 respectively.

Hence we get,

$$\begin{aligned} C_{D_{o,TO}} &= 0.044 \\ C_{D,TO} &= 0.0482 \\ C_{D,G} &= 0.0392 \end{aligned}$$

$$\begin{aligned} C_{L,R} &= \frac{1}{2}mgSV^2 \\ V_r &= 1.1V_{Stall}, V_{stall} = 10\text{m/s}, V_r = 11\text{m/s} \\ C_{L,R} &= 0.0134 \text{ (W/S)} \end{aligned}$$

$$P = 0.5$$

$$V_{TO} = 1.2 V_{Stall} = 12 \text{m/s}$$

Based on this approach, we find that the W/S for our configuration (W=7.83kg P=444.36Watt) is about 1.47kg/m<sup>2</sup>.

Alternatively,

Wing loading for loiter can be converted to takeoff conditions by dividing the loiter wing loading by the ratio of the average of loiter weight to takeoff weight. In our case the weight of the UAV does not change, hence this ratio can be assumed to be 1.0. [19]

$$\left(\frac{W}{S}\right)_{takeoff} = \frac{W_{takeoff}}{W_{loiter}} \left(\frac{W}{S}\right)_{loiter} \quad (3.2.2)$$

[28]

$$\left(\frac{W}{S}\right)_{takeoff} = 1 \cdot 30.76 = 30.76 \text{kg/m}^2$$

Taking the higher value among the two approaches we estimate the wing loading for take off condition to be 30.76 kg/m<sup>2</sup>.

### 3.2.2 Wing Loading for Climb Rate

For a propeller aircraft a higher wing loading results in higher cruise speeds but lower takeoff and climb rates. Whereas a lower wing loading results in slower cruise speeds but higher takeoff and climb rates. We also know propellers are more efficient at lower speeds. [28] Since we intend to get off the ground quick, we thus take a generous Climb Angle of 12° and make our following estimate.

$$\left(\frac{W}{S}\right)_{ROC_{max}} = \frac{1}{\sin\gamma} \left( \frac{\eta_p^2}{\left(\frac{W}{P}\right)_{ROC_{max}}} \rho \sqrt{\frac{3C_{D_0}}{K}} - \frac{1.155}{\left(\frac{L}{D}\right)_{max}} \right) \quad (3.2.3)$$

[28] where,

$\gamma$  (climb angle) = 12° (10° - 30°) [28],  $\eta_P$  (Propeller Efficiency) = 0.5,  $C_{D_0}$  = 0.04, AR = 8.3, e = 0.81,  $k = \frac{1}{\pi e A R} = 0.0471$ ,  $\rho = 1.17 \text{ kg/m}^3$ ,  $(L/D)_{max}$  value of 19.4824.

$$\left(\frac{W}{S}\right)_{ROC_{max}} = \frac{1}{0.2078} \cdot \left( \frac{0.25}{\frac{7.83 \cdot 9.81}{2009.7}} \cdot 1.17 \cdot \sqrt{\frac{0.12}{0.0471}} - \frac{1.155}{19.4824} \cdot 1.56 \right) = 33.6525 \text{N/m}^2$$

$$\left(\frac{W}{S}\right)_{ROC_{max}} = 3.4304 \text{kg/m}^2$$

### 3.2.3 Wing Loading for Stall

We can calculate the wing loading for stall conditions by first considering force balance in the vertical direction for a steady level flight  $L = W$ . Thus, we get [19]

$$\left(\frac{W}{S}\right)_{stall} = \frac{1}{2} \rho v_{stall}^2 C_{L_{max}} \quad (3.2.4)$$

[19]

where,

$v_{stall} = 10 \text{ m/s}$ ,  $\rho = 1.17 \text{ kg/m}^3$ ,  $C_{L_{max}} = 1.56$ , as based from our previous estimates and design conditions tabulated at the start of the section.

$$\left(\frac{W}{S}\right)_{stall} = \frac{1}{2} \cdot 1.17 \cdot 10^2 \cdot 1.56 = 91.26 \text{N/m}^2$$

$$\left(\frac{W}{S}\right)_{stall} = 9.30 \text{kg/m}^2$$

### 3.2.4 Wing Loading for Cruise

For cruising conditions at steady level flight, we know that  $L = W$ .

$$\left(\frac{W}{S}\right)_{cruise} = \frac{1}{2} v_{cruise}^2 C_{L_{max}} \quad (3.2.5)$$

[19] We are required to maximise the range and hence our aerodynamic efficiency or Lift-to-Drag ratio  $L/D = C_L/C_D$  for a propeller aircraft to calculate the wing loading. Thus, for the given conditions,  $\frac{d(C_L/C_D)}{dC_L} = 0$ , we get[19],

$$C_{D_o} = \left( \frac{1}{\pi e AR} \right) C_L \quad (3.2.6)$$

[19]

$$C_L = \sqrt{\pi e A R C_{D_o}} = \sqrt{\pi \cdot 0.81 \cdot 8.3 \cdot 0.04} = 0.9191$$

Using this value in equation 3.2.6, we get

$$\left( \frac{W}{S} \right)_{cruise} = \frac{1}{2} \cdot 1.17 \cdot 18^2 \cdot 0.9091 = 172.31 \text{ N/m}^2$$

$$\left( \frac{W}{S} \right)_{cruise} = 17.56 \text{ kg/m}^2$$

### 3.2.5 Wing Loading for Absolute Ceiling

Also considering the performance of our UAV at it's absolute ceiling, which we have set at 100m, which gives us a reasonable tolerance limit from our actual design altitude of 80m, we can arrive at a wing loading using the following relation[28]

$$\left( \frac{W}{P} \right)_{AC} = \frac{\sigma_{AC}}{\frac{R O C_{AC}}{\eta_P} + \sqrt{\frac{2}{\rho_{AC} \frac{3 C_{D_o}}{K}} \left( \frac{W}{S} \right) \left( \frac{1.155}{\left( \frac{L}{D} \right)_{max} \eta_P} \right)}} \quad (3.2.7)$$

[28] where,

$$\eta_P \text{ (Propeller Efficiency)} = 0.5, \rho_{AC} = 1.16 \text{ kg/m}^3 \text{ (150m)}, \sigma_{AC} \text{ (Relative Air Density)} = 0.975, \\ C_{D_o} = 0.04, \text{AR} = 8.3, e = 0.81, k = \frac{1}{\pi e AR} = 0.0471, C_{L_{max}} = 1.56$$

Using the power calculation from previous analysis and the calculated values of the constants, we can get an approximate value as

$$\left( \frac{W}{P} \right)_{AC} = \frac{7.3548^2}{\left( \frac{W}{P} \right)_{AC}^2} = \frac{7.3548^2}{\left( \frac{7.83 \cdot 9.81}{113} \right)^2} = 117.06 \text{ N/m}^2$$

$$\left( \frac{W}{S} \right) = 11.93 \text{ kg/m}^2$$

### 3.2.6 Wing Loading for Loiter

As we are designing our Mini UAV for surveillance, which requires periods of time during which it loiters, we would like to calculate an optimum wing loading estimate that would optimize this period of loiter. The wing loading should be selected to provide high L/D.

$$\left( \frac{W}{S} \right)_{loiter} = \frac{1}{2} \rho v_{loiter}^2 C_{L_{loiter}} \quad (3.2.8)$$

[28] For a propeller aircraft, the maximum power condition for this phase is achieved when  $C_L^{\frac{3}{2}}/C_D$  ratio is maximised. For this condition,  $\frac{d(C_L^{\frac{3}{2}}/C_D)}{dC_L} = 0$ , we get[19]

$$C_{D_o} = \frac{1}{3} \left( \frac{1}{\pi e AR} \right) C_L^2 \quad (3.2.9)$$

[28]

$$C_L = \sqrt{3 \pi e A R C_{D_o}} = \sqrt{3 \cdot \pi \cdot 0.81 \cdot 8.3 \cdot 0.04} = 1.5920$$

Using this value in equation 3.2.9, we get

$$\left( \frac{W}{S} \right)_{loiter} = \frac{1}{2} \cdot 1.17 \cdot 18^2 \cdot 1.5920 = 301.75 \text{ N/m}^2$$

$$\left( \frac{W}{S} \right)_{loiter} = 30.76 \text{ kg/m}^2$$

### 3.2.7 Wing Loading Selection

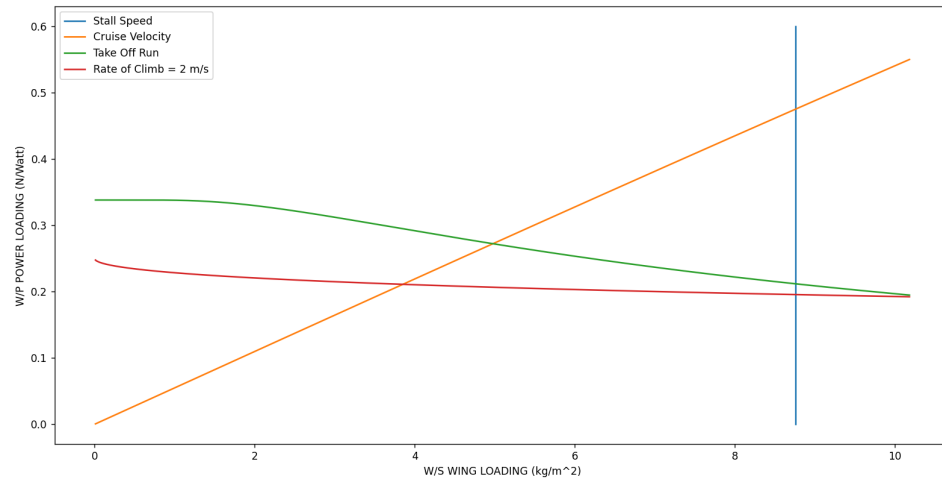
Sl. No.	Mission Segment	Wing Loading ( $\text{kg}/\text{m}^2$ )
1	Takeoff	30.76
2	Climb Rate	3.4304
3	Cruise	17.56
4	Loiter	30.76
5	Stall	9.30
6	Absolute Ceiling	11.93

Table 3.2.2: Wing Loading at different Flight Conditions

### 3.2.8 Power Loading vs Wing Loading Plot

Below, we've roughly plotted our Power Loading vs Wing Loading for different phases of our flight, which might come in handy and give us a sanity check as we revise our design for the Power Required and the corresponding Wing Loading that we choose.

Parameters used to arrive at these plots have been tabulated at the beginning of the Section.



## Chapter 4

# Second Weight Estimate

13.4

Using the weights from previous calculations, the weight estimation process estimates our Final Total weight  $W_o$  and our Empty Weight Fraction. ( Payload Weight = 2.0 kg, Powerplant Weight = 2.27 kg) We then calculate a  $W_o$  estimate from the equation given below

$$W_o = \frac{W_{payload} + W_{powerplant}}{1 - \frac{W_{empty}}{W_o}} \quad (4.0.1)$$

[28] which initially gives a value of  $W_o = 8.2084$  kg. After that we substitute the estimated  $W_o$  into the design curve equation that we fit previously and get an estimated Empty Weight Fraction

$$\frac{W_{empty}}{W_o} = 1.206 * W_o^{-0.3} \quad (4.0.2)$$

[28] Using this new empty weight fraction, we again use equation 4 to estimate  $W_o$ . This process is iterated a few more times, and converges at iteration number 8 where we get a final estimate of Total Weight,  $W_o = 8.8017$  kg and an Empty Weight Fraction of 0.5337. Given below is the plot for second weight estimate against the number of iterations.

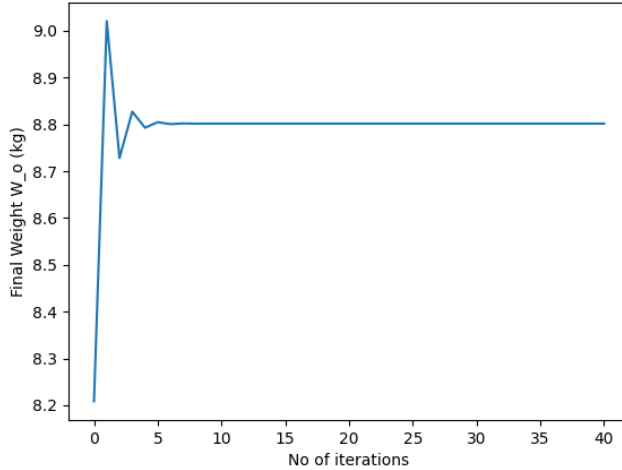


Figure 4.0.1: Second Weight Estimate

# Chapter 5

## Wing Design

In this section, we initially estimate the required Lift Coefficients for some of the important phases of the mini UAV mission profile. Accordingly, multiple airfoils are considered using data available on popular airfoil databases, and consequently simulated using the XFLR5 software. The performance plots are inspected, and multiple wing configurations are also conceptually fabricated and simulated after considering multiple wing design parameters and elements such as the chord length, span length, high lift devices(flaps), taper ratio and sweep angle. After arriving at the performance plots which closely outline the set design specifications and considering the practical feasibility of design, a final airfoil and wing configuration is chosen and represented.

### 5.1 Design Lift Coefficient Calculations

Here we first re-estimate the lift coefficients that shall be referred to when searching an airfoil and drafting the wing.

#### 5.1.1 Cruise

The most important stage of the mission profile is the Cruise Phase. We design the mini UAV to cruise at an altitude of  $100\text{ m}$  at a velocity of  $18\text{ m/s}$ . It is desirable to chose a wing which has the best aerodynamic performance during this phase of the flight i.e. The Lift-to-Drag Ratio is maximum at the operating Lift Coefficient desired for cruise. Hence, firstly the Lift Coefficient for cruise at  $100\text{ m}$  is calculated.

Cruise Velocity :  $v_{cruise} = 18\text{ m/s}$

Density at  $100\text{ m}$  :  $\rho_{100m} = 1.21\text{ kg/m}^3$

Wing Loading :  $\frac{W}{S} = 90\text{ N/m}^2$

$$C_{Lcruise} = \frac{W}{\frac{1}{2}\rho_{100m}v_{cruise}^2 S} \quad (5.1.1)$$

Thus, the lift coefficient for cruise is  $C_{Lcruise} = 0.46$ .

#### 5.1.2 Stall

The Stall Characteristics of the UAV is very important to take into consideration as it gives a physical cap on the performance that can be extracted out of the conceptual wing ( $C_{Lmax}$ ). Considering a stalling range of  $v_{stall} = 10\text{ m/s}$  to  $10.5\text{ m/s}$ , the stall lift coefficients are calculated at  $100\text{ m}$  altitude.

$$C_{Lstall} = \frac{W}{\frac{1}{2}\rho_{100m}v_{stall}^2 S} \quad (5.1.2)$$

Thus, the lift coefficient for stall is  $C_{Lstall} = 1.48$  for  $v_{stall} = 10\text{ m/s}$  and  $C_{Lstall} = 1.35$  for  $v_{stall} = 10.5\text{ m/s}$ .

### 5.1.3 Take-Off

During take-off, usually a higher lift coefficient is beneficial for a shorter take-off distance and a faster rate of climb and is helpful in considering the using of high lift devices to increase the  $C_{Lmax}$  of the wing. Hence, the Take-Off Lift Coefficient is estimated.

Take Off Velocity :  $v_{to} = 1.1 \times v_{stall} = 11m/s$

Wing Loading :  $\frac{W}{S} = 90N/m^2$

Sea Level Density :  $\rho_{sl} = 1.225kg/m^3$

$$C_{L_{to}} = \frac{W}{\frac{1}{2}\rho_{sl}v_{to}^2S} \quad (5.1.3)$$

Thus, the lift coefficient for the desired climb profile is  $C_{L_{to}} = 1.21$

### 5.1.4 Climb

It is essential to also take into account the climb characteristics of the UAV before finally arriving at the selection of the airfoil.

The Accelerated lift coefficient requirements is taken into account as the UAV takes off and is lifted to the design altitude of 100 m. A load factor of  $n = 1.8$  is considered and the climb lift coefficient is calculated.

Climb Velocity :  $v_{climb} = 13m/s$

Averaged Density :  $\rho = 1.22kg/m^3$

Load Factor :  $n = 1.5$

Wing Loading :  $\frac{nW}{S} = 162N/m^2$

$$C_{L_{climb}} = \frac{W}{\frac{1}{2}\rho v_{climb}^2 S} \quad (5.1.4)$$

Thus, the lift coefficient for the desired climb profile is  $C_{L_{climb}} = 1.31$

The estimated wing lift coefficients that will be referred to for the mission profile are tabulated below.

$C_L$	Values
$C_{Lcruise}$	0.46
$C_{Lstall}$	1.35-1.48
$C_{L_{to}}$	1.21
$C_{L_{climb}}$	1.31

## 5.2 Airfoil Selection

Using XFLR5, with our calculated design  $C_l$ , we generated the following table with airfoil data of some airfoils.

Airfoil	Zero lift Angle of Attack	$C_{l_{max}}$	$stall$	$C_{l_\alpha}$ (per radian)	$(C_l/C_d)_{max}$	$\alpha^\circ$ for $(C/D)_{max}$
NACA15013	-1	1.230	14	0.082	63.302	7
NACA25012	-2.5	1.370	12	0.095	69.139	9
NACA34012	-2.5	1.469	13.5	0.100	62.117	10
GOE 553	-2	1.52	14	0.93	150	4

Table 5.2.1: Airfoil Data

A crude estimation is done which helped in identifying the required airfoil section lift coefficient  $C_l$  by employing a scaling of 0.9 on the wing lift coefficient  $C_L$  i.e.  $C_{l_{max}} = \frac{C_{L_{max}}}{0.9} = 1.44$  and  $C_{l_{cruise}} = \frac{C_{L_{cruise}}}{0.9} = 0.51$ . It is also noted that the airfoil was selected with a design lift coefficient corresponding to the Lift-to-Drag Max condition i.e. Highest Aerodynamic Efficiency.

After thoroughly investigating of the available airfoil datasets as given in bigfoil.com and airfoiltools.com, further simulating in XFLR5 and based on the requirements tabulated, the *GOE 553* airfoil has been chosen for the UAV design. Figure 5.2.1, shows the profile of the selected airfoil *GOE 553*.

### Airfoil GOE 553

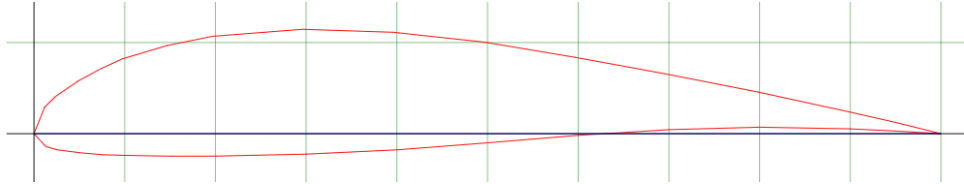


Figure 5.2.1: Plot of chosen Airfoil GOE 553

Table 5.2.2: Geometric and Aerodynamic Characteristics GOE 553

Geometric Characteristics	Value	Aerodynamic Characteristics	Value
Camber	4.7% of chord	$C_{l_{max}}$	1.52
Chord Length	0.34 m	$stall$	14°
Location of maximum camber	39.6% of chord from LE	$(L/D)_{max}$	100
Maximum Thickness	13.7% of chord		

### Operational Characteristics of Airfoil

We first estimate the chord length and span length of the wing. We set the Aspect Ratio at 8.3 as found previously, the Wing loading at  $90N/m^2$  and the weight of the UAV at  $8.8kg$ . Employing the relation

$$AR = \frac{b^2}{S} \quad (5.2.1)$$

The Span length is estimated to be  $b = 2.82m$ . Accordingly assuming a rectangular wing, the chord length is estimated at  $c = 0.34m$ .

For assessing the performance of the aerofoil for our UAV, we compare its performance in the target design atmospheric conditons of Cruise. For our cruise altitude of  $100m$  with a cruise velocity of  $18m/s$  and assuming ISA conditons, we get, density of air () as  $1.21562\text{ kg}/m^3$ , viscosity of air of  $1.809 \times 10^{-5}\text{ Ns}/m$ , and the operating Reynolds number has been estimated to be which is used for finding operational characteristics.

$$Re = \frac{\rho vc}{\mu} \quad (5.2.2)$$

Reynolds number of airfoil : 415000

The following image shows the graphs obtained during analysis on XFLR5 including the airfoil Drag Polar, Lift vs  $\alpha$  curve, Pitching Moment vs  $\alpha$  and Lift-to-Drag vs  $Cl$ .

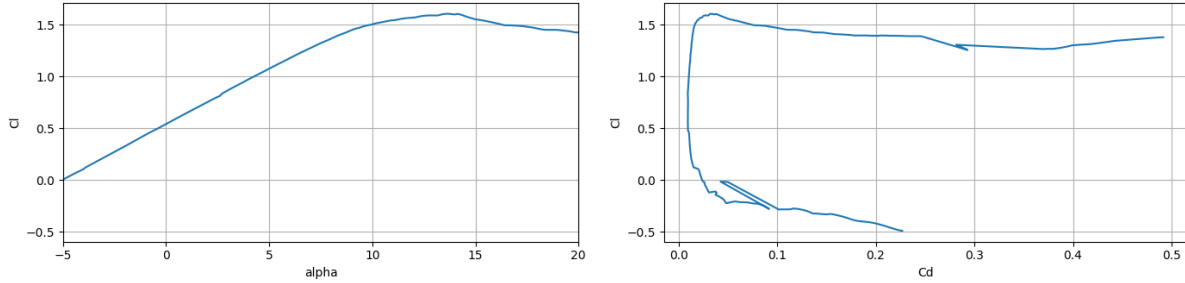


Figure 5.2.2: Airfoil Lift vs Angle of Attack and Drag Polar

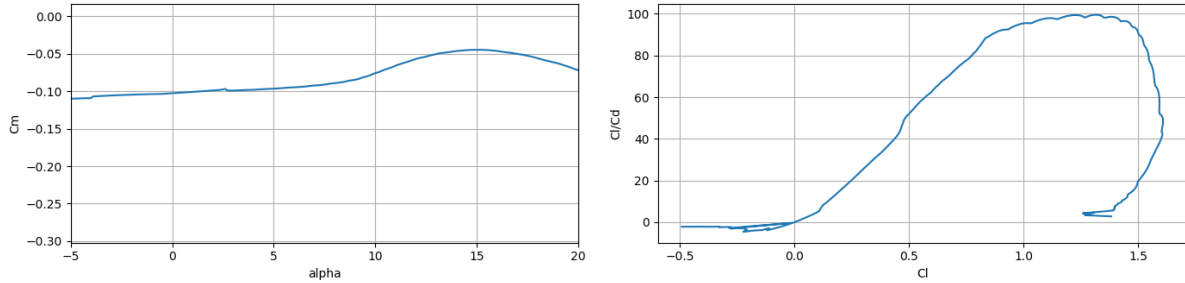


Figure 5.2.3: Airfoil Moment vs Angle of Attack and Airfoil Lift-To-Drag vs Lift Coefficient

From the Plots, it is observed that the Design  $C_l$  of the Airfoil is at 0.7, while it reaches a max Lift-to-Drag of 100. The  $C_{l\text{stall}} = 1.52$  and it stalls at  $\alpha = 14^\circ$ . The Moment Coefficient has a positively increasing slope with no jumps which can be fixed by the design of an effective tail, and the drag polar has also been found to be referred to for later drag analysis. All of this indicate values close to the design specifications, and thus a wing has been conceptually fabricated and simulated.

### Operational Characteristics of Wing

To finalize the selection of the airfoil, a rectangular wing is made using the airfoil and the estimated Span Length  $b = 2.82 \text{ m}$  and chord length  $c = 0.34 \text{ m}$ , and the operational characteristics have been simulated at the calculated operational  $Re = 415000$ .

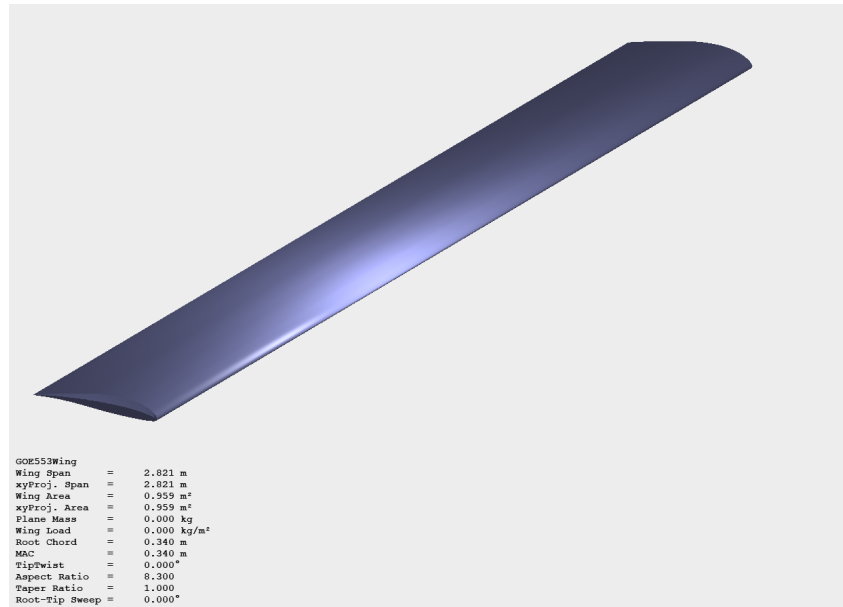


Figure 5.2.4: 3D image of rectangular wing for chosen airfoil

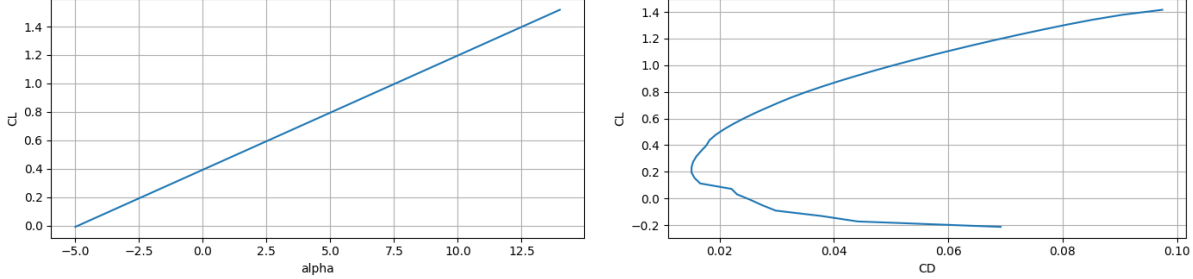


Figure 5.2.5: Wing Lift vs Angle of Attack and Wing Drag Polar

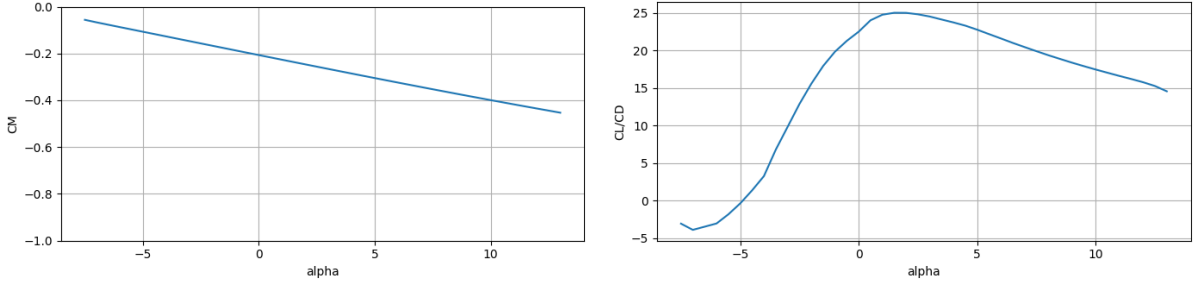


Figure 5.2.6: Wing Lift-To-Drag vs Angle of Attack

From the Plots, it is observed that the max Lift-to-Drag occurs at  $\alpha = 1^\circ$ , at which the operating  $C_L = 0.48$ , which agrees with the design requirements for cruise. But it is also noted that the max Lift-to-Drag decreases to 25, which is expected as compared to the airfoil. The  $C_{Lstall} = 1.45$  and it stalls at  $\alpha = 14^\circ$ , which agrees with the design requirement for Stall. The Moment Coefficient has a positively increasing slope with no jumps which can be fixed by the design of an effective tail, and the drag polar has also been found to be referred to for later drag analysis.

But we also note that the airfoil does not produce high lift at lower angle of attacks. Thus flaps have been designed to take into consideration the take-off and initial climb requirements. After a few trial and errors in XFLR5, the following wing with flaps is obtained.

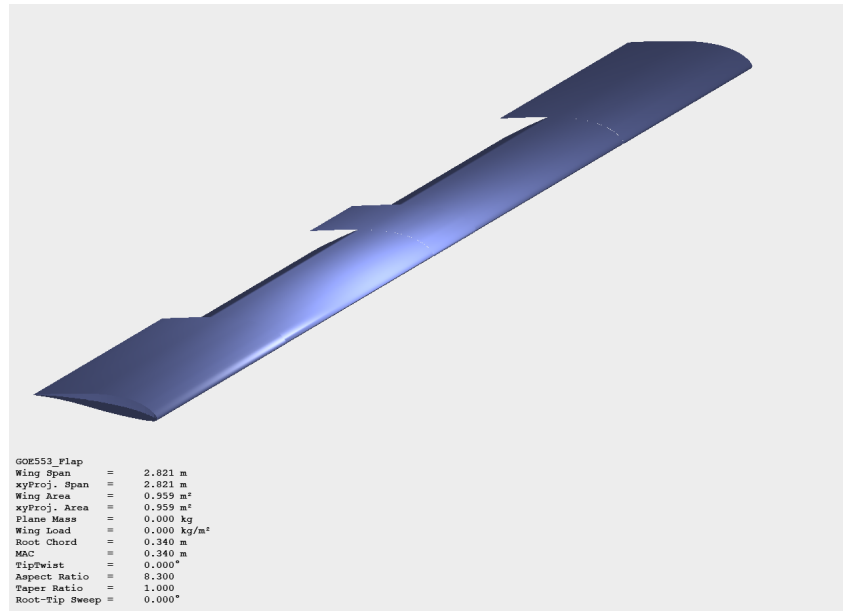


Figure 5.2.7: Wing with Flap

The Flap is taken at from  $0.6 \times c$ , and the flap length is taken along the span from  $0.1m$  to  $0.8m$ , keeping a healthy distance for the later roll considerations and aileron considerations. Simulating the flow with

the flap deflection at  $\delta = 20^\circ$ , the new lift curve slope is plotted.

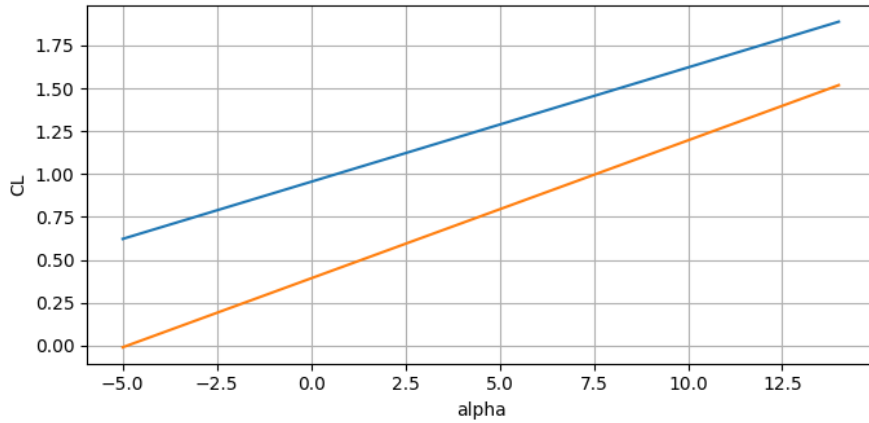


Figure 5.2.8: Wing Lift vs Angle of Attack with and without flaps

It is observed that the Lift increases, and we get the take off and climb design  $C_L = 1.21$  to  $1.31$  at angle of attacks  $\alpha = 3^\circ$  to  $6^\circ$ , which is very desirable. Thus the flaps will be operational during take-off and accelerated climb.

### 5.3 Angle of Incidence

During the flight, the drag should be kept to a minimum for optimal fuel consumption. When the fuselage is at zero angle of attack, the drag is at its lowest. However, with this arrangement, the wings ought to provide sufficient lift to sustain the aircraft's weight. To do this, the wing is attached to the fuselage at an angle that causes the wings to produce the necessary lift while the fuselage is at a zero angle of attack. We refer to this angle as the incidence angle ( $i_w$ ).

The design lift coefficient corresponding to the cruise is

$$C_{L,design} = \frac{W}{\frac{1}{2}\rho_{100m}v_{cruise}^2 S} \quad (5.3.1)$$

The incidence angle is calculated from the design lift coefficient as follows

$$C_{L,design} = C_L (i_{w0}) \quad (5.3.2)$$

where  $C_L$  and  $i_{w0}$  are the lift curve slope of the wing and zero lift angle of attack of the wing respectively, which can be obtained from the airfoil lift curve slope ( $C_l$ ) and zero lift angle ( $i_l$ ) as follows

$$i_{w0} = i_l + J \quad (5.3.3)$$

$$C_L = \frac{C_l}{1 + \frac{C_l}{AR}} \quad (5.3.4)$$

where  $J$  is the twist angle and  $J = -0.4$  can be used for an approximate estimate.

Using the parameters of the airfoil selected and a twist of  $0^\circ$ , the angle of incidence comes out to be  $i_w = 1^\circ$ . This is chosen as it corresponds to the angle of attack  $\alpha$  for Design Lift Coefficient for Cruise.

### 5.4 Taper Ratio

The taper ratio () is defined as the ratio between the tip chord ( $C_t$ ) and the root chord ( $C_r$ ). [28]

$$\lambda = \frac{C_t}{C_r} \quad (5.4.1)$$

The theoretically best aerodynamic efficiency ( $\delta = 0$ ) and lowest induced drag are obtained with a wing platform that is elliptical in planform shape with no twist. This wing shape gives an elliptical span wise

aerodynamic loading (i.e., lift per unit span) and uniform downwash over the wing, which, as previously mentioned, is theoretically the minimum induced drag condition, and so  $\delta = 0$ . However, this value is unobtainable in any practical wing design. [29]

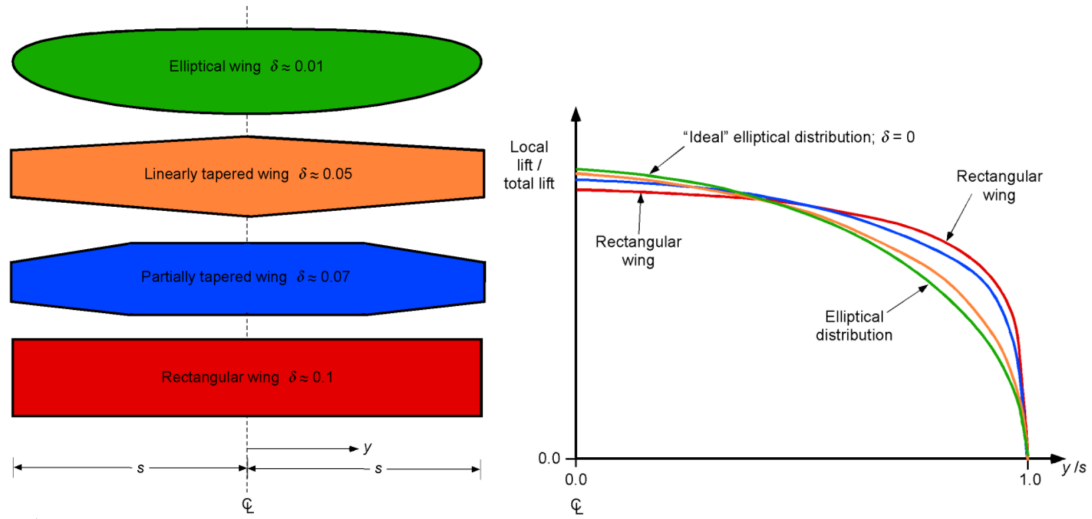


Figure 5.4.1: Different taper ratios for a wing and their  $C_L$  variation [29]

Based on the above analysis and our mission requirements, we realise that the having a Taper would improve the aerodynamic characteristics of our UAV. The same has been analysed below. A tapered wing with taper ratio = 0.6 is conceptually crafted, and recalculating the span and root chord lengths to  $b = 3.0\text{ m}$  and  $c_{root} = 0.4\text{ m}$  to get the same aerodynamic plots and wing area as obtained for the rectangular wing.

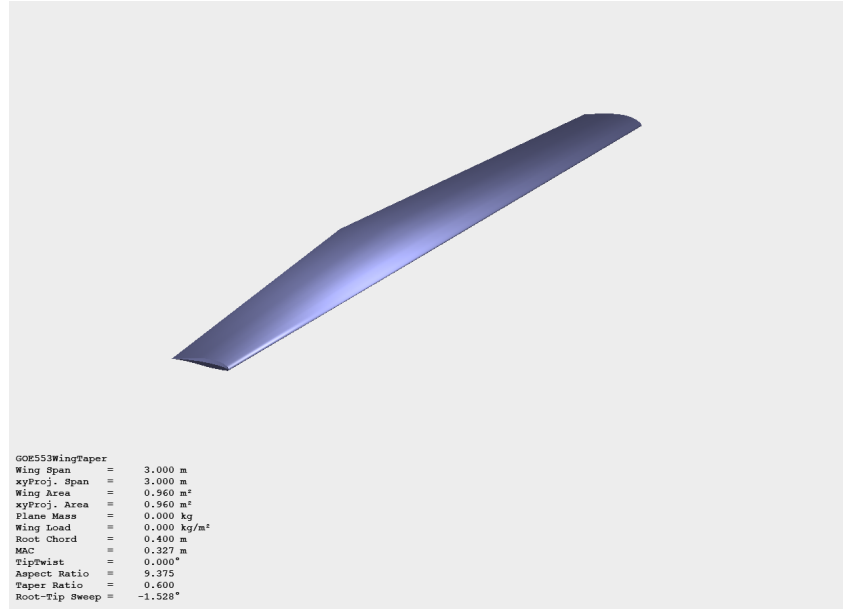


Figure 5.4.2: Tapered Wing with taper ratio 0.6

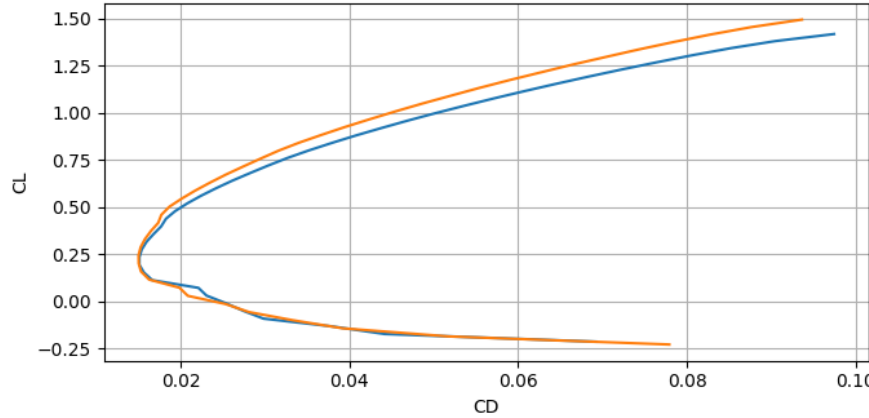


Figure 5.4.3: Drag Polar of wing with and without taper

All aerodynamic operational characteristics are similar, but plotting the drag polar, it is observed we get the same lift for reduced drag values for the tapered wing. We also compare the streamlines over both rectangular and tapered wing.

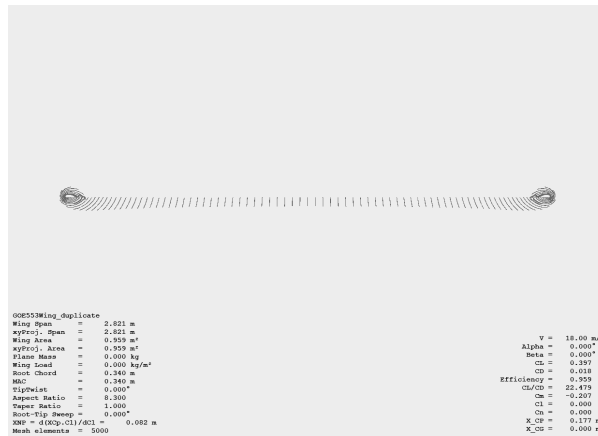


Figure 5.4.4: Air Stream over Rectangular Wing

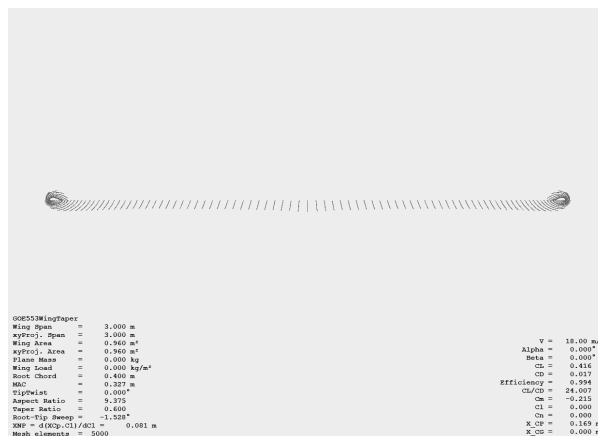


Figure 5.4.5: Air Stream over Tapered Wing

From the pictures of the streamlines over the 2 wings, it is observed that the Induced drag is lesser for the tapered wing as the wing tip vortices size decreases for a tapered wing, and thus a tapered wing

configuration could be beneficial.

However, considering, the practical difficulties in fabrication and weighing it against the marginal improvements in the aerodynamic characteristics, we have chosen not to add a taper and hence have decided to proceed with a rectangular wing.

## 5.5 Sweep Angle

The quarter-chord line sweep angle  $c/4$  and the leading-edge sweep angle LE are the two significant sweep angles. Because the leading edge should be swept beneath the Mach cone to minimize wave drag, the leading-edge sweep angle is the most important one for supersonic aircraft. When discussing high-speed subsonic aircraft that are close to the speed of sound, the sweep angle of the quarter-chord line,  $c/4$ , is important. Based on the relationship, the leading edge sweep angle LE often lowers the drag divergence Mach number( $M_D$ ). It is the Mach number at which an airfoil's aerodynamic drag starts to increase quickly as the Mach number rises. the relation between LE and MD is approximately given by

$$\frac{1 - (M_D)}{1 - (M - D)_{=0}} = 1 - \frac{c}{90} \quad (5.5.1)$$

where,  $(MD)$  and  $(MD)=0$  drag divergence Mach number of swept and unswept wing respectively. When the drag divergence Mach number is higher than 0.6, it usually corresponds to the transonic regime. Our UAV operates far below the transonic region, with a cruising velocity of about 18m/s and a Mach number of about 0.1. Hence at this stage, the requirement of a sweep angle is not found to be necessary. In other words,  $LE = 0$  and  $c/4 = 0$ .

## 5.6 Wing Configuration

### Low-Wing Configuration

Advantages :

- Stability: Low-wing UAVs tend to have better lateral stability, making them more stable during flight, which can be advantageous for various missions, including surveillance and mapping.
- Payload Capacity: The low-wing design allows for larger payload capacity, as the payload can be mounted beneath the fuselage without interference from the wings.
- Aerodynamic Efficiency: Low-wing UAVs can benefit from reduced interference drag between the wings and the fuselage, leading to improved overall aerodynamic efficiency and potentially longer endurance.
- Ease of Ground Operations: The low-wing configuration can facilitate easier ground operations, such as launching and landing, especially in confined spaces, as the wings are not obstructing the ground clearance.

Disadvantages :

- Vulnerability to Ground Debris: The positioning of the wings beneath the fuselage makes low-wing UAVs more vulnerable to debris on the ground during takeoff and landing, potentially leading to damage to the wings or payload.
- Limited Ground Clearance: Low-wing UAVs may have limited ground clearance, which could be problematic when operating in rough terrain or on uneven surfaces.
- Visibility: While low-wing configurations offer good visibility for the payload, they may have slightly reduced visibility for certain types of sensors or cameras mounted on top of the fuselage.
- Maintenance Accessibility: Accessing components located beneath the fuselage, such as the payload or landing gear, may require more effort and time compared to configurations with the wings positioned higher.

## **Mid-Wing Configuration**

Advantages :

- Balanced Lift Distribution: Mid-wing UAVs typically achieve a balanced lift distribution, enhancing stability and control during flight maneuvers.
- Aerodynamic Efficiency: Similar to low-wing configurations, mid-wing UAVs can benefit from reduced interference drag between the wings and the fuselage, contributing to overall aerodynamic efficiency.
- Visibility: Mid-wing designs provide good visibility for both sensors and cameras mounted on top of the fuselage, allowing for effective surveillance and reconnaissance missions.
- Payload Flexibility: The mid-wing configuration allows for flexible payload integration options, as the payload can be mounted on top of the fuselage without interference from the wings.
- Ground Clearance: Mid-wing UAVs typically have sufficient ground clearance for landing gear and other components, making them suitable for various terrain conditions.

Disadvantages :

- Complexity: Mid-wing configurations may involve more complex structural design and integration, especially when considering payload mounting and aerodynamic considerations.
- Maintenance Accessibility: Accessing components located on top of the fuselage, such as sensors or cameras, may require additional effort and time compared to configurations with the wings positioned lower.
- Vulnerability to Damage: The mid-wing position exposes the wings to potential damage during ground operations, such as takeoff and landing, especially in rough terrain.
- Weight Distribution: Achieving optimal weight distribution in mid-wing UAVs can be challenging, as the payload and other components need to be carefully balanced to maintain stability and performance.

## **High-Wing Configuration**

Advantages :

- Excellent Visibility: High-wing UAVs provide unobstructed visibility for sensors, cameras, and other payloads mounted beneath the fuselage, facilitating effective surveillance and reconnaissance missions.
- Stability: High-wing configurations typically offer greater inherent stability, especially during banking maneuvers, making them suitable for various applications, including aerial mapping and monitoring.
- Protection from Ground Debris: With the wings positioned above the fuselage, high-wing UAVs are less susceptible to damage from ground debris during takeoff and landing, enhancing durability and reliability.
- Payload Flexibility: High-wing designs allow for flexible payload integration options, as the payload can be mounted beneath the fuselage without interference from the wings.
- Ease of Ground Operations: High-wing UAVs often feature ample ground clearance, making takeoff and landing operations easier, especially in rough or uneven terrain.

Disadvantages :

- Aerodynamic Interference: High-wing configurations may experience increased interference drag between the wings and the fuselage, potentially impacting overall aerodynamic efficiency and endurance.

- Limited Maneuverability: While high-wing UAVs offer stability, they may have slightly reduced maneuverability compared to other configurations, which can be a consideration for certain mission profiles.
- Weight Distribution: Achieving optimal weight distribution in high-wing UAVs can be challenging, as the payload and other components must be carefully balanced to maintain stability and performance.
- Complexity in Payload Integration: Mounting certain payloads, such as gimbals or sensors, beneath the fuselage of high-wing UAVs may require more complex integration and mounting solutions compared to configurations with the wings positioned lower.

Based on the above considerations and keeping in mind our mission requirements, the **High Wing design** is most suitable.

## 5.7 Dihedral Angle

The dihedral angle refers to the upward angle between the wings of the aircraft when viewed from the front or rear. Traditionally, dihedral angles are employed in fixed-wing aircraft for various aerodynamic benefits like

- **Roll Stability:** When the UAV is tilted due to a disturbance, such as wind gusts or turbulence, the dihedral angle generates a restoring moment.
- **Adverse Yaw Reduction:** When an aircraft rolls, there is a tendency for the nose to yaw in the opposite direction of the turn. Dihedral angles create differential drag between the wings, which counters this adverse yaw effect, making the UAV more responsive and easier to control during turns.
- **Improved Lift-to-Drag Ratio:** By reducing induced drag caused by wingtip vortices, the aircraft becomes more efficient in generating lift.

For ease of manufacturing we are not taking any dihedral angle. This can change depending on our calculations for stability of aerodynamic characteristics of our UAV.

## 5.8 Aileron

A hinge moment is involved in the deflection of any control surface, including the aileron. The aerodynamic moments known as hinge moments are what need to be overcome in order to deflect the control surfaces. The amount of the enhanced pilot force needed to move the appropriate actuator in order to deflect the control surface is determined by the hinge moment. In order to reduce the actuation system's size and cost, the ailerons should be engineered with the lowest possible control forces.

We do these calculations after stability analysis.

# Chapter 6

## Fuselage Design

We now proceed with the design of the aircraft's fuselage. The Fuselage plays a pivotal role in the aircraft, serving as the primary housing for the payload and propulsion system. The design parameters in the design process involves the following:-

### 6.1 Fuselage Length

The fuselage length is estimated by using data on similar aircraft. The fuselage length is obtained as a function of:

$$L = aW_0^c \quad (6.1.1)$$

Where,  $L$  is the fuselage length,  $W_0$  is the MTOW, and  $a$  and  $c$  are parameters obtained by fitting the curve.

Following aircraft are chosen for best fit curve:

UAV	Weight - $W_0$ (kg)	Fuselage Length - $L$ (m)
Sitaria E UAV	35	2.8
JOUAV CW-0015	20	2.06
BLueShark F250	13.5	1.26
JOUAV CW-007	7.8	1.3

Table 6.1.1: Fuselage Lengths for different UAVs

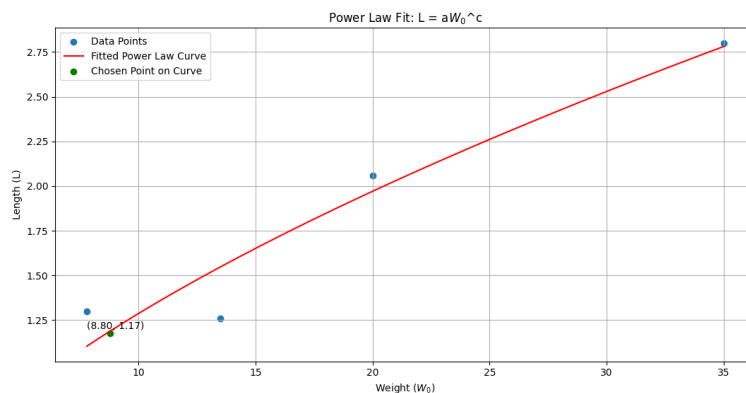


Figure 6.1.1: Fuselage Length Estimation

Based on the best-fit plot using a MATLAB code 13.7, we obtained values of  $a = 0.3117$  and  $c = 0.6156$  for the parameters. For the design weight  $W_0 = 8.8$  kg, the fuselage length is calculated using the relation as shown below.

$$\text{Fuselage Length} = 0.3117 \times (8.8)^{0.6156} = 1.17 \text{ m}$$

Therefore, the design fuselage length is approximately **L = 1.17 m**

## 6.2 Fuselage Sizing

The fuselage defines the aircraft's shape and influences its aerodynamics during flight. It acts as a central hub for assembling the various aircraft components and evenly distributes forces across its entire surface. Our focus will be on sizing the fuselage to accommodate the volume needs of our payload.

Our payload primarily includes the camera, with the fuselage also containing the propulsion system. The propulsion system comprises the battery, motors, wiring, flight navigation, guidance, and communication electronics.

Below are the estimated dimensions of the fuselage components:

Components	Dimensions (in mm <sup>3</sup> )
T Motor	185 × 125 × 105
Tattu 16000mAh Battery	190 × 75 × 63
Workswell WIRIS Integrated Thermal and Optical Sensor	76 × 107 × 102
Prana Air SQUAIR Weather Sensor	58 × 25 × 46
Flight Controller with GPS module	50 x 40 x 30
Gimbal	124.3 × 106 × 133.3
Miscellaneous	100 × 100 × 100

The arrangement of the above components is done inside the fuselage keeping the following in mind:

1. The *motor* has been sized keeping in mind the specific kV rating as per our thrust requirement.
2. Our *camera* has been sized keeping in mind the 6 DOF motion and the gimble size.
3. Our battery has been sized based off the energy density for our specific mAh rating, allowing for BMS.
4. The payload other than the camera, such as the guidance and navigation as well as the communication electronics.

As a second layer of protection for the internal components in case of turbulence , there will be a 1cm layer of foam on the inside. For deciding the final dimensions of the fuselage, we have taken the following tolerance levels so that there is a minimum spacing gap between the components, and also the ease of movement if required:

$$\begin{aligned} \text{Radial Tolerance} &= 5\% \\ \text{Axial Tolerance} &= 10\% \end{aligned}$$

By following the above guidelines, we arrive at the arrangement roughly depicted in the following figure

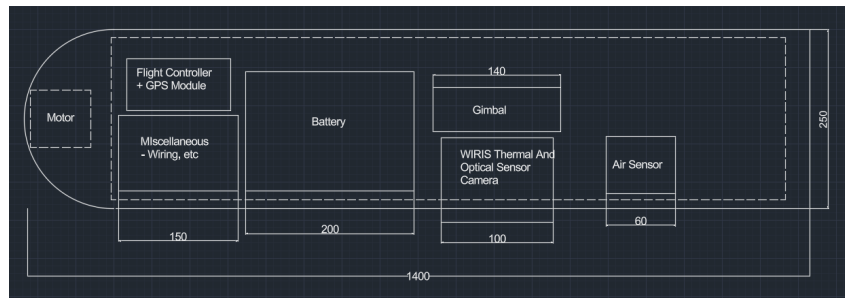


Figure 6.2.1: Components Arrangement in Fuselage

The components shown in the figure have been designed considering,

- The total fuselage length is taken to be close to the values predicted by fitting a curve to similar aircraft data based on MTOW.
- The nose of the fuselage is taken as spherical for simplicity and for decreased drag.
- The motor, flight controller and batteries are arranged such that wire length is minimised and wiring is convenient.
- The sensors are placed such that they can be used optimally.

Following these requirements and the figure of the arrangement, the initial sizing of our fuselage are:

Length	1.400 m
Fuselage Diameter	0.250 m
Width	0.200 m

Table 6.2.1: Fuselage Dimensions

The arrangement and sizing can change based on our CG calculations.

# Chapter 7

## Tail Design

### 7.1 Tail Configuration

#### Low-Tail Configuration

Advantages :

- Ground Clearance: With the tail positioned low, there is ample ground clearance during takeoff, landing, and taxiing, reducing the risk of ground strikes and potential damage to the tail assembly.
- Stability: Low tail configurations often provide enhanced stability, particularly in pitch control, which can be advantageous for maintaining flight stability during various mission profiles, including surveillance and mapping.
- Payload Accessibility: Mounting the tail low allows for easier access to the payload bay or cargo area, simplifying payload integration and maintenance procedures.
- Protection from Damage: Placing the tail low reduces its exposure to damage from airborne debris or obstacles, contributing to the overall durability and reliability of the UAV.
- Reduced Aerodynamic Interference: Low tail configurations minimize interference drag between the tail and the fuselage, improving overall aerodynamic efficiency and potentially extending flight endurance.

Disadvantages:

- Limited Maneuverability: Low tail configurations may have slightly reduced maneuverability compared to other tail configurations, particularly in pitch control, which could impact the UAV's ability to perform agile maneuvers.
- Vulnerability to Ground Debris: Despite reduced exposure to damage from airborne debris, low tail configurations remain vulnerable to ground debris during takeoff and landing, potentially leading to damage to the tail assembly.
- Weight Distribution Challenges: Achieving optimal weight distribution in low-tail UAVs can be challenging, as the position of the tail may affect the UAV's center of gravity and stability characteristics.
- Potential for Ground Strikes: Despite the advantages of ground clearance, low tail configurations may still be susceptible to ground strikes, particularly when operating in rough terrain or uneven surfaces

#### Mid-tail Configuration

Advantages:

- Balanced Stability: Mid-tail configurations provide a balanced distribution of control surfaces, offering good stability and control authority during flight maneuvers, especially in pitch control.

- Payload Protection: Placing the tail at a mid-position above the fuselage can provide some protection for payloads mounted beneath the UAV, reducing the risk of damage from ground debris during takeoff and landing.
- Ground Clearance: Mid-tail configurations typically offer sufficient ground clearance for the tail, reducing the risk of ground strikes during taxiing, takeoff, and landing operations.
- Aerodynamic Efficiency: Mid-tail configurations can contribute to improved aerodynamic efficiency by minimizing interference drag between the tail and the fuselage, leading to better overall performance and endurance.
- Maneuverability: Mid-tail configurations can provide good maneuverability and control authority, allowing for precise flight control and navigation, especially in challenging environments.

**Disadvantages:**

- Complexity: Mid-tail configurations may involve more complex design and integration processes compared to other tail configurations, potentially increasing manufacturing costs and maintenance requirements.
- Weight Distribution: Achieving optimal weight distribution in mid-tail UAVs can be challenging, as the position of the tail may affect the UAV's center of gravity and stability characteristics.
- Aeroelastic Effects: The mid-tail position may be susceptible to aeroelastic effects, such as flutter or vibrations, which could affect the UAV's structural integrity and flight performance.
- Height Restrictions: The mid-tail position may impose limitations on the overall height of the UAV, which could be a consideration for operations in confined spaces or environments with low clearance.

## **High-tail Configuration**

**Advantages:**

- Stability: High tail configurations offer improved stability during flight, especially in pitch control, which can be beneficial for various missions such as surveillance and mapping.
- Protection of Payload: Placing the tail above the fuselage can protect the payload, such as sensors or cameras, from ground debris during takeoff and landing, enhancing the durability and reliability of the UAV.
- Reduced Risk of Ground Strikes: With the tail positioned higher, there is less risk of the tail striking the ground during takeoff, landing, or taxiing operations, reducing the potential for damage to the UAV.
- Enhanced Aerodynamic Efficiency: High tail configurations can contribute to improved aerodynamic efficiency by reducing interference drag between the tail and the fuselage, leading to better overall performance and endurance.
- Improved Maneuverability: High tail configurations can provide better control authority and maneuverability, especially in pitch control, which can be advantageous for performing precise flight maneuvers or navigating challenging terrain.

**Disadvantages:**

- Complexity: High tail configurations may involve more complex design and integration processes, potentially increasing manufacturing costs and maintenance requirements.
- Weight Distribution: Achieving optimal weight distribution in high-tail UAVs can be challenging, as the position of the tail may affect the UAV's center of gravity and stability characteristics.
- Height Limitations: The higher tail position may impose limitations on the overall height of the UAV, which could be a consideration for operations in confined spaces or environments with low clearance.

- Vulnerability to Wind: High tail configurations may be more susceptible to wind-induced disturbances, such as turbulence or gusts, which could affect flight stability and control, especially in adverse weather conditions.

Based on the above and considering our mission requirements and stability requirements based on design of wing, we have chosen to have **Low tail or Conventional tail configuration**.

## 7.2 Optimum Tail Arm

Two very significant aircraft general design requirements are aircraft low weight and low drag. Both of these may be combined and translated as the requirement for a low aircraft wetted area. To estimate the effectiveness of the horizontal tail, an optimum tail arm needs to be found. This would serve as an initial estimate. As the horizontal tail arm is increased, the fuselage wetted area is increased, but horizontal tail wetted area is decreased. Also, as the horizontal tail arm is decreased, the fuselage wetted area is decreased, but horizontal tail wetted area is increased. Hence, we are looking to determine the optimum tail arm to minimize drag; which in turn means to minimize the total wetted area of the aft portion of the aircraft.

$V_H$  value is generally low for high maneuverability common values of 0.2 for fighter jets are considered whereas for stability as values as high as 1.1 are taken. So, based on our mission profile we take  $V_H = 1$  [28]

Value of  $l_{opt}$  was calculated (using equation 6.46 in [28])

$$l_{opt} = \sqrt{\frac{4CSV_H}{\pi D_f}} \quad (7.2.1)$$

$l_{opt}$  was found out to be 1.137 m. A correction factor is added to compensate for our assumption of conical fuselage denoted as  $K_c$ . For a cylindrical fuselage it's value is 1.4. The corrected  $l_{opt}$  is 1.159 m.

## 7.3 Horizontal Tail

A preliminary analysis for the horizontal tail to obtain the **horizontal tail area estimate and aspect ratio** is done by first considering the Wing Moment Coefficient vs Angle of Attack plot.

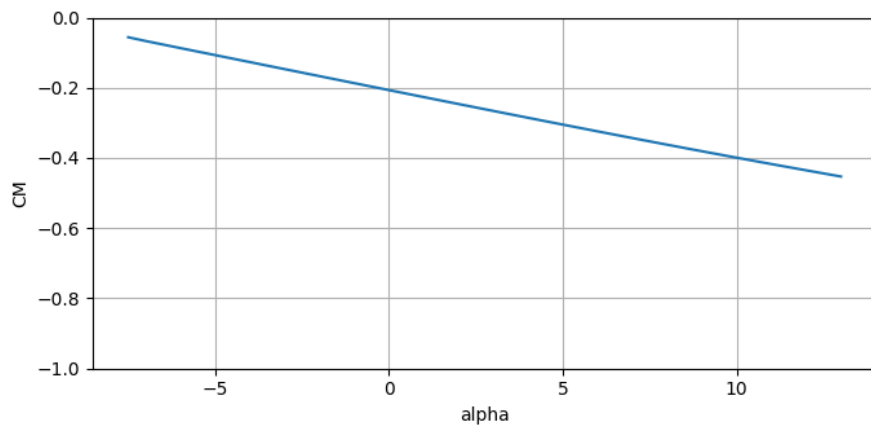


Figure 7.3.1:  $C_M$  vs  $\alpha$  for Wing

It's observed that at  $\alpha = 0$ ,  $C_{M_o} = -0.2$ , and the moment curve slope is  $C_{M_\alpha} = -0.02$  per  $^\circ$ . For Static Stability,  $C_{M_o} > 0.0$  and  $C_{M_\alpha} < 0$ , and a more statically stable plane will have a more negative moment curve slope. For a conceptual horizontal tail area sizing, the moment equations denoting contributions from the tail is considered.

$$C_{M_{cg\,tail}} = \eta V_H C_{L_{\alpha\,tail}} (i_w + \epsilon_o - i_t) - \eta V_H C_{L_{\alpha\,tail}} \alpha_w \left(1 - \frac{d\epsilon}{d\alpha}\right) \quad (7.3.1)$$

[28] where  $V_H = \frac{S_t l_t}{S_w c_w}$ ,  $i_t$  and  $i_w$  are the tail and wing setting angles, and the downwash angle is  $\epsilon = \epsilon_o + \frac{d\epsilon}{d\alpha} \alpha$ . Now again, it is seen that the 1st term in the equation changes the  $C_{M_\alpha}$  of the plane, while the 2nd term changes  $C_{M_\alpha}$ .

The original wing coefficient of moment graph can be formulated by the equation

$$C_M = -0.2 - 0.02\alpha \quad (7.3.2)$$

[28] From [28], front mounted propeller wing tail arm is usually about 60% of the fuselage length (1.4m). Thus tail arm  $l_t = 0.84m$ .

Now taking  $l_t = 0.84m$ ,  $S_w = 0.96m^2$ ,  $c_w = 0.34m$ ,  $AR_w = 8.3$ ,  $i_w = 1^\circ$ ,  $i_t = -3^\circ$  and approximating downwash angle and downwash slope as  $\frac{d\epsilon}{d\alpha} = \frac{2C_{L\alpha_{wing}}}{\pi AR_w} = 0.34$  and  $\epsilon_o = \frac{2C_{L\alpha_{wing}}}{\pi AR_w} = 1.73^\circ$  where  $C_{L\alpha_{wing}} = 0.08/\text{deg}$  and  $C_{L\alpha_{wing}} = 0.4$  from the wing  $C_L$  vs  $\alpha$  plots, the tail area is varied and hence  $V_H$  is varied and the resultant total moment coefficient is plotted for different  $V_H$ .

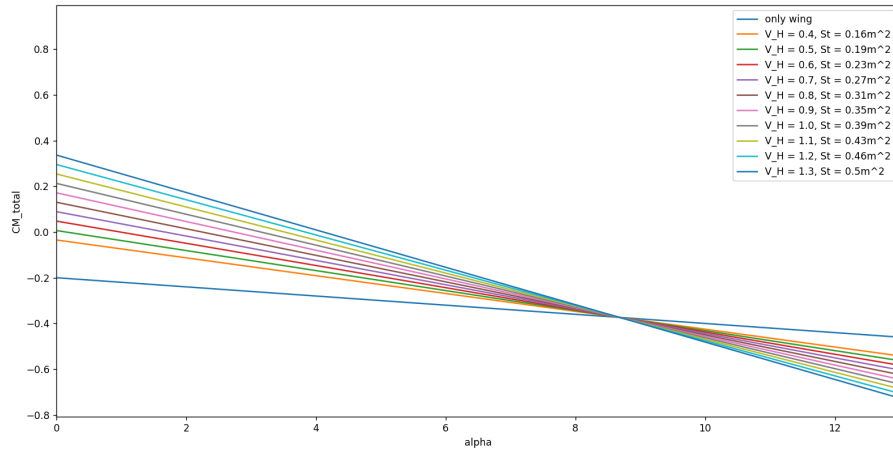


Figure 7.3.2: Total  $C_M$  vs  $\alpha$  for Varying  $V_H$  and Tail Area ( $S_t$ )

It is noted that  $C_{M_\alpha} = 0$  for the wing + tail configuration at  $V_H = 0.5, S_t = 0.16m^2$ , and keeps increasing as the tail area and hence  $V_H$  is increased, and subsequently the  $C_{M_\alpha}$  slope becomes increasingly negative. Thus from the above plot, it is desirable if we choose the tail area in the range of  $0.27 - 0.45m^2$  for a subsequent  $V_H$  of  $0.7 - 1.2$ , keeping a tail setting angle  $i_t = -3^\circ$ . The code to generate the plot has been added to the appendix.

An initial **Aspect Ratio** can be chosen for the tail by using the relation given in [28]

$$AR_t = \frac{2}{3} AR_w \quad (7.3.3)$$

Thus, given the selected Wing Aspect Ratio  $AR_w = 8.3$ , a preliminary Tail Aspect Ratio is chosen as  $AR_t = 5.0$ . Accordingly, the span length and chord for the tail (selected rectangular for ease of manufacturing) can be found from the equation

$$b_t = \sqrt{AR_t S_t} \quad c_t = \frac{S_t}{b_t}$$

Thus for an  $AR_t = 5.0$  and  $S_t = 0.27 - 0.45m^2$ , a span length range of  $b_t = 1.16 - 1.5 m$  and a chord length range of  $c_t = 0.23 - 0.3 m$ .

Considering our mission requirements and the design parameters estimated in this section, we have chosen a symmetric NACA 0014 airfoil for the horizontal tail.



Figure 7.3.3: Airfoil for Tail: Symmetric Airfoil NACA0014

## 7.4 Vertical Tail

The vertical tail parameters must be determined initially such that the directional stability requirements are satisfied. In later stages of the vertical tail design process, the directional trim requirements and directional control requirements will be examined.

As we are in early stage of the vertical tail design, where other aircraft components have not been designed, the vertical tail moment arm is selected to be equal to the horizontal tail moment arm ( $l_{opt} = l_V$ ). This assumption means that the vertical tail is located at the same distance from the wing as the horizontal tail.

Similar to the horizontal tail volume coefficient, a new parameter that is referred to as the vertical tail volume coefficient ( $V_V$ ) is defined. If the value of this parameter is close to the ballpark number, we are 90% sure that the directional stability requirements have been satisfied. A typical value for the vertical tail volume coefficient is between 0.02 and 0.12.[28] Vertical planform area is calculated as follows;

$$S_V = \frac{bSV_V}{l_V} \quad (7.4.1)$$

Based on the design parameters and assuming a value of 0.04 for  $V_V$  (Table 6.4) [28], we get  $S_V = 0.13 m^2$ .

Considering our mission requirements and the design parameters estimated in this section, we have chosen a symmetric NACA 0014 airfoil for the vertical tail with a chord( $c_V$ ) of 0.4m and span ( $b_v$ ) of 0.325m.

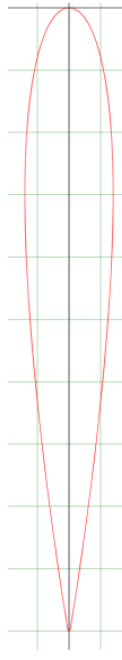


Figure 7.4.1: Airfoil of Vertical Tail

# Chapter 8

## Landing Gear Design

The landing gear, a crucial component of aircraft design, supports the aircraft on the ground during taxiing, takeoff, and landing. For an appropriate design of a landing gear system for our UAV, we shall be describing the following parameters of the Landing gear.

- Configuration
- Fixed or retractable
- Landing Gear Geometry
- Load on each strut
- Tire sizing
- Nose Wheel Steering

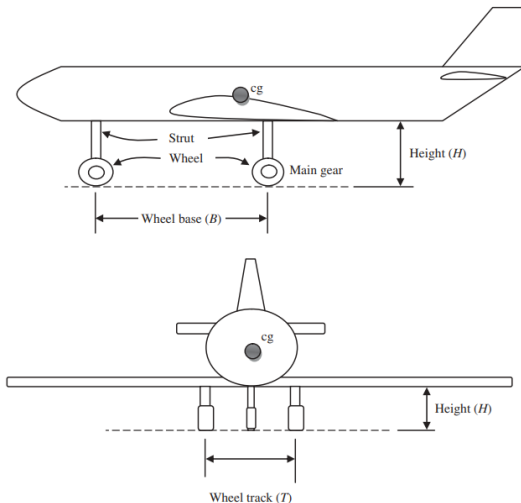


Figure 8.0.1: Landing Gear Parameters [28]

### 8.1 Landing gear Configuration

Based on our CG and design specifications, the **Tricycle LG** is the best fit. The Tricycle LG is the most widely used landing gear configuration. Figure 8.1.1 shows the Tricycle Landing gear in a typical aircraft. The wheels aft of the aircraft cg are very close to it (compared with forward gear) and carry much of the aircraft weight and load; Two main gears are at the same distance from the cg in the x-axis and the same distance in the y-axis (left and right sides); thus both carry the same load. The forward gear is far from the cg (compared with the main gear); hence it carries a much smaller load. The share of the main gear from the total load is about 80–90%, so the nose gear carries about 10–20%.

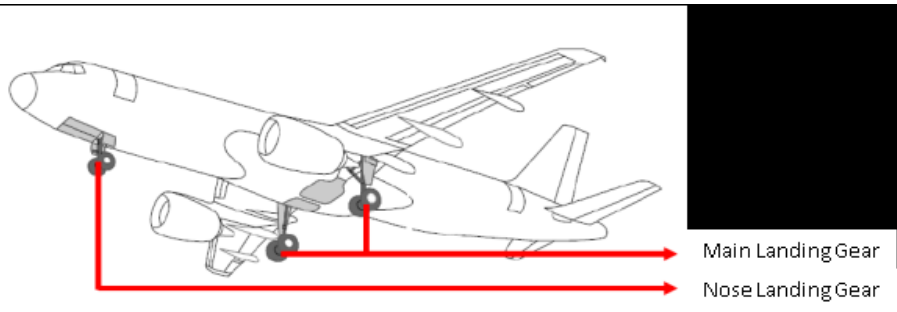


Figure 8.1.1: Tricycle Landing Gear

## 8.2 Landing Gear retraction

As a major design configuration for our Mini UAV is low weight and low cost it is prudent to design a Fixed Landing gear setup so as to reduce the cost and weight. A general assessment of the same is presented below.

No.	Item	Fixed (non-retractable) landing gear	Retractable landing gear
1	Cost	Cheaper	Expensive
2	Weight	Lighter	Heavier
3	Design	Easier to design	Harder to design
4	Manufacturing	Easier to manufacture	Harder to manufacture
5	Maintenance	Easier to maintain	Harder to maintain
6	Drag	More drag	Less drag
7	Aircraft performance	Lower aircraft performance (e.g., maximum speed)	Higher aircraft performance (e.g., maximum speed)
8	Longitudinal stability	More stable (stabilizing)	Less stable (destabilizing)
9	Storing bay	Does not require a bay	Bay must be provided
10	Retraction system	Does not require a retraction system	Requires a retraction system
11	Fuel volume	More available internal fuel volume	Less available internal fuel volume
12	Aircraft structure	Structure is uninterrupted	Structural elements need reinforcement due to cutout

Figure 8.2.1: Comparison of Fixed vs Retractable system

Also, since the maximum speeds to be attained by the Mini UAV are relatively low, the need for retraction of the Landing Gear is not envisaged.

## 8.3 Landing Gear Geometry

### 8.3.1 Position of Main LG and Nose LG

From our design specifications and fuselage design, we have a fuselage length fixed to 1.2m. Based on the distribution of the loads within the fuselage, we have our CG location to be about 40% of the total length. That is about 0.68m from the nose. Considering a CG margin of 10% of the total length of the fuselage, we get the **fwd most CG point to be about 0.51m** and the **aft CG point to be about 0.85m**. The figure below describes these specifications graphically.

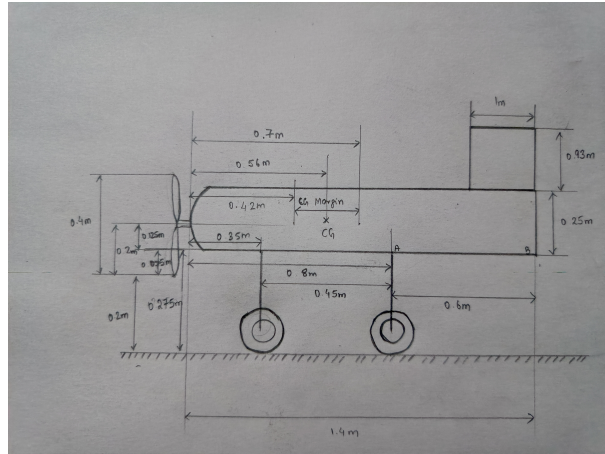


Figure 8.3.1: Landing Gear Design

Based on these specifications we have chosen our nose gear to be ahead of the forward CG point and the Main gear to be behind the aft CG point as shown above. Hence the distance of the Nose LG from the nose has been chosen to be about 0.35m and the main LG from the nose has been chosen to be about 0.9m. This gives us a **wheel base of 0.55m**.

### 8.3.2 Landing Gear Track

The next parameter to be defined in the geometry is the track of the wheels. (As per 9.5.3 of Sadrey[28] the landing gear track is usually set as a percentage of the wingspan or the width of the fuselage. For small UAVs, the track is typically 15% to 20% of the wingspan. This ensures adequate stability during taxiing, takeoff, and landing, without making the gear too wide. Since our wing span is about 2.82m for this span, we have chosen a wheel track of **0.423m** ( $0.75\text{m} \times 2$ ).

### 8.3.3 Landing Gear Height

With the position of the main LG and nose LG properly defined, we can now determine the landing gear height requirements. For which it is essential to first understand the parameters that define the Landing Gear height. The two main conditions for the determination of the LG height are as listed below,

1. Aircraft General Ground Clearance Requirement
2. Take-Off Rotation Ground Clearance Requirement

We shall now look at each of these in detail.

#### Aircraft General Ground Clearance Requirement

One of the primary functions of the landing gear is to protect the aircraft structure from the ground. This job is performed by providing a clearance from the ground. The clearance is measured from the lowest point of the aircraft to the ground. In our case, the prop tip will be the lowest point nearest to the ground.

As a general rule (As per 9.5.1.2 of Sadrey[28]), for a propeller aircraft we take a clearance of 0.2m from the propeller tip as the height of the Landing gears. As per our design, we have a fuselage diameter of 0.23m with a propeller diameter of 0.406m as depicted in Fig 8.3.1. Applying the 0.2m ground clearance to these design specifications, we get the **landing gear height from the fuselage to be 0.24355m**.

#### Take-Off Rotation Ground Clearance Requirement

An aircraft is usually rotating about the main gear in order to increase the lift to prepare for take-off (see Figure 8.3.2). This is also true for landing operation, in which the aircraft rotates to gain a high angle of attack. Since our aircraft is nose gear, the height of the landing gear must be set so that the

tail or rear fuselage does not strike the ground during the take-off rotation or landing with a high angle of attack.

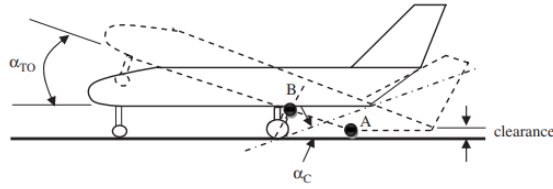


Figure 8.3.2: Take off Ground Clearance

The take-off rotation ground clearance requirement to prevent a fuselage hit is as follows:

$$\alpha_C \alpha_{TO}$$

where the clearance angle is,

$$\alpha_C = \tan^{-1} \left( \frac{H_f}{AB} \right) \quad (8.3.1)$$

[19]

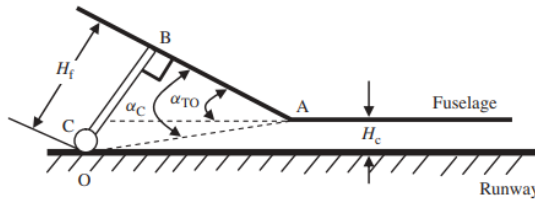


Figure 8.3.3: Clearance Angle Estimation

From our design specifications,  $H_f$  is **0.275m** and  $AB$  as **0.6m** as depicted in Fig 8.3.1. Hence the **clearance angle would be 24.65°**. In our case the **take off angle is about 12°** and hence our design ensures that the tail would not touch during take off or landing.

### 8.3.4 Landing Gear Overturn Angle

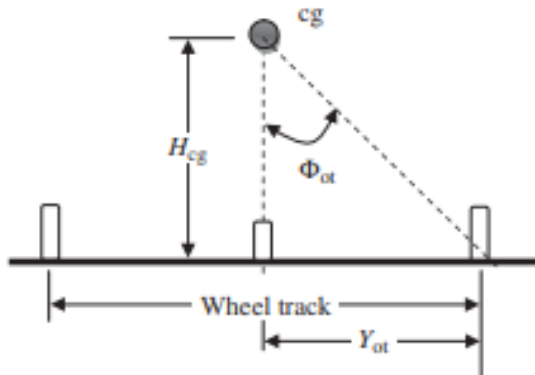


Figure 8.3.4: Estimation of Overturn Angle

The wheel track of the Landing Gear Design main wheel should be arranged so that the aircraft cannot roll over too easily due to wind or during a ground turn. The overturn angle is the angle which is critical to the aircraft overturn. To determine the overturn angle, look at the aircraft front view, the angle

between the vertical line passing through the aircraft cg and the line between the aircraft cg and that of the main wheels is the overturn angle (As shown in Fig 8.3.4) . In the figure, the parameter Hcg is the height of the aircraft cg from the ground. As a rule of thumb, the wheel track must be such that the overturn angle ( $\phi_{ot}$ ) is inside the following recommended limit:

$$\phi_{ot} \geq 25^\circ$$

Based on our dimensions we find that the overturn angle( $\phi_{ot}$ ) is 69.86 Deg. Which meets the stability condition for overturn criteria.

## 8.4 Load on each Landing Gear

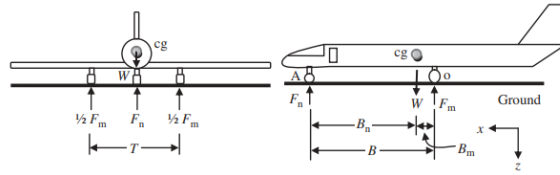


Figure 8.4.1: Loads acting on the LG

Figure 8.4.1 shows a stationary aircraft with a tricycle landing gear on the ground. The aircraft weight (W) is carried by three wheels (i.e., two main and one nose gear). Due to the ground mobility (i.e., steering) requirement, typically the nose gear must not carry less than about 5% of the total load and also must not carry more than about 20% of the total load (e.g., aircraft weight). Thus, the main gear carries about 80–95% of the aircraft load. The loads on nose and main gears are denoted by  $F_n$  and  $F_m$  respectively.

Calculation of the static loads on each gear is performed by employing equilibrium equations. Since the aircraft is in static equilibrium, the summation of all forces in the z direction must be zero:

$$\Sigma F_z = 0 \quad F_n + F_m = W$$

Furthermore, the summation of all moments about O is zero

$$\Sigma M_o = 0 \quad F_{n_B} \cdot W_{B_m} = 0$$

Applying the above equations with our design specifications as depicted in Fig 8.3.1. We find the **Load on the Nose LG is 13.81N** and that being applied on the main LG is 72.52N (**Each main LG will have a load of 36.26N**). This implies that the nose LG carries a load of about 16% and the main LG carries about 84% of the total load. These specifications also ensure good ground mobility of the mini UAV.

## 8.5 Selection of Tyres

Based on our load calculations, design parameters, ground clearance requirements, extensive market survey and based on tyres being utilized by UAVs of similar weight and dimensions we have selected a *3.5 inch PU tyre*. The main features of the same are as follows:-

- Core made of bore retrofitted copper pipe, force balanced and wear-resistant
- Golden Aluminum Hub
- Size: 3.5inch
- Weight: 68g

## 8.6 Nose Wheel Steering System

Considering the maneuvering requirement during taxi, minor course adjustments to be catered for during take off roll and landing run the team has chosen to use a Nose Wheel Steering system. The nose wheel will have a freedom of rotation of 45 Deg and enable the aircraft to efficiently maneuver on ground. The nose wheel steering will be connected to the flight controller to enable its control on ground.

# Chapter 9

## Three View Diagram

As individual parts of the UAV have been designed, it is now time to make a 3-D model of the UAV.

### 9.1 CAD Model of UAV

The 3D model of the UAV has been made and is as shown below.



Figure 9.1.1: Isometric View



Figure 9.1.2: Front View

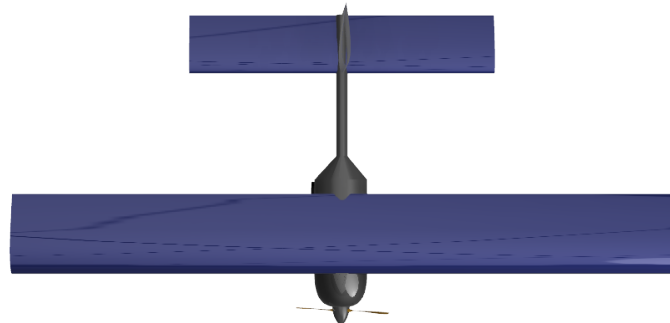


Figure 9.1.3: Top View

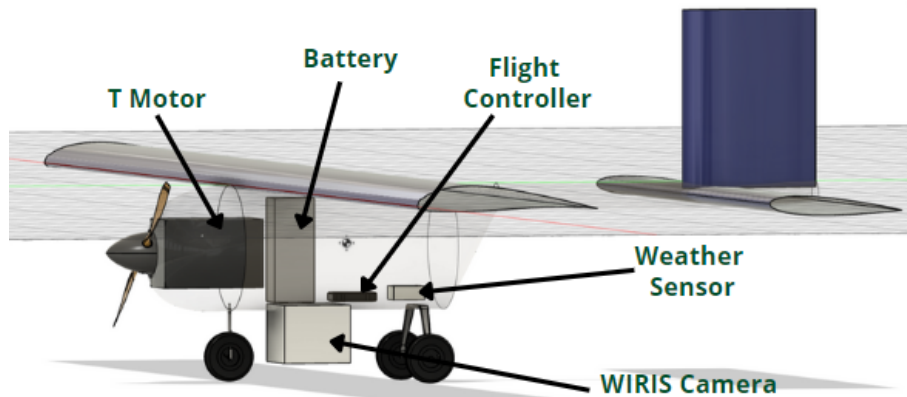


Figure 9.1.4: Components

## 9.2 Centre of Gravity

The centre of gravity is 220 mm behind and 109 mm the wing leading edge.

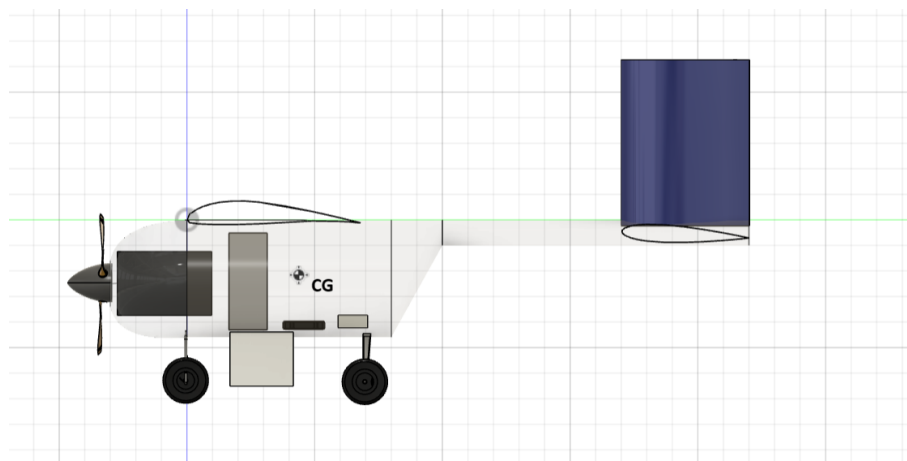


Figure 9.2.1: CG

The centre of gravity is 177 mm behind and 111 mm the wing leading edge.

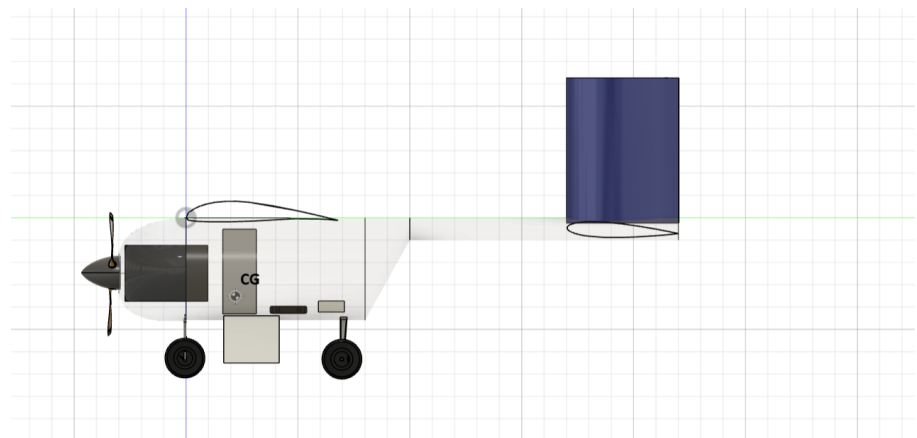


Figure 9.2.2: CG without Wing

# Chapter 10

## Stability Analysis

### 10.1 Simulation Analysis

#### 10.1.1 Modelling the UAV

For stability analysis, the UAV was crafted on the XFLR5 software which included the wing, vertical tail, horizontal tail and an approximated fuselage.

Initially the wing, horizontal and vertical tail were modelled and the CG was taken into account from the initial design of the plane as shown previously, and small adjustments were made to the vertical stabilizer and the tail arm to account for stability as well as adjusting the CG. The fuselage was then additionally modelled to take into account the fuselage's effect on the stability parameters and especially to check for high wing roll stability. The Simulations were conducted at altitude 100 m and  $V_\infty = 18$  m/s, at  $Re \approx 415000$ .

After creating the initial model, several adjustments were made to stabilize the aircraft :

- A high wing configuration was used
- A dihedral angle of  $2^\circ$  was given to boost roll stability and counter possible disbalancing gusts and turbulent flow as experienced above forest cover
- The length of the bulk of fuselage was extended to add directional and roll stability and reduce Dutch Roll oscillations observed in previous iterations of our design
- The tail arm length was extended to boost longitudinal stability
- The horizontal stabilizer was given a  $2^\circ$  setting angle to match trim  $\alpha_{trim} = \alpha_{design}$  for design  $C_L$

Name	Values
Wing Chord, Horizontal Tail Chord, Vertical Tail Chord	(0.34 m, 0.28 m, 0.35 m)
Wing Span, Horizontal Tail Span, Vertical Tail Span	(2.82 m, 1.5 m, 0.4 m)
Wing Area, Horizontal Tail Area, Vertical Tail Area	(0.96 m <sup>2</sup> , 0.42 m <sup>2</sup> , 0.14 m <sup>2</sup> )
Wing Dihedral Angle $\Lambda$	$2^\circ$
Tail Arm $l_t$	1.2 m
Horizontal Tail Setting Angle $i_t$	$2^\circ$
Total Fuselage Length	1.7 m
Fuselage Diameter	250 mm
CG Location (from Nose) $X_{CG}$	0.5 m
NP Location (from Nose) $X_{NP}$	0.57 m
Wing AC Location (From Nose) $X_{AC_w}$	0.325 m
Tail AC Location (From Nose) $X_{AC_t}$	1.46 m

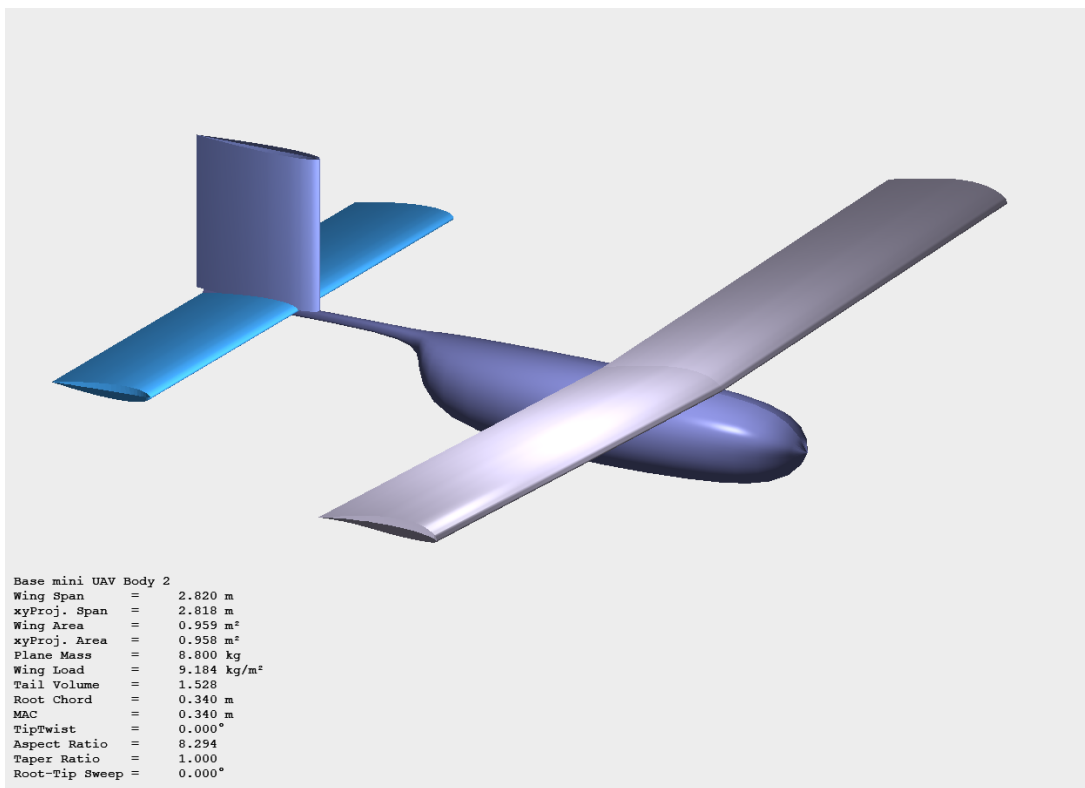


Figure 10.1.1: XFLR5 UAV Model Isometric View



Figure 10.1.2: XFLR5 UAV Model Front View

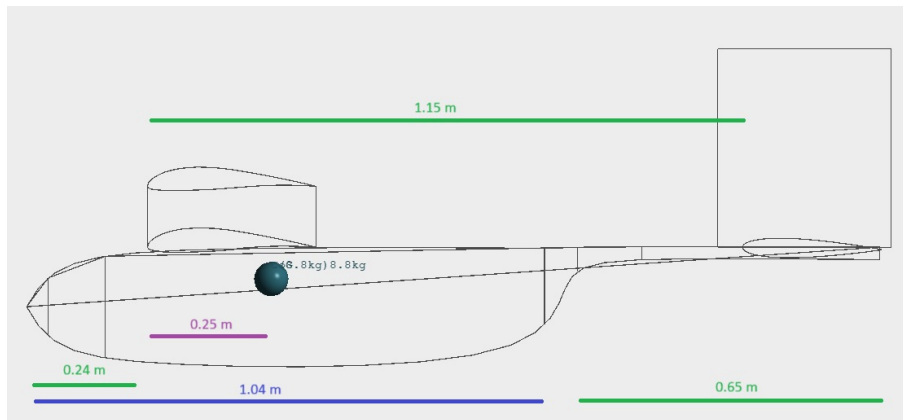


Figure 10.1.3: XFLR5 UAV Side View with sizings

### 10.1.2 Simulation Results

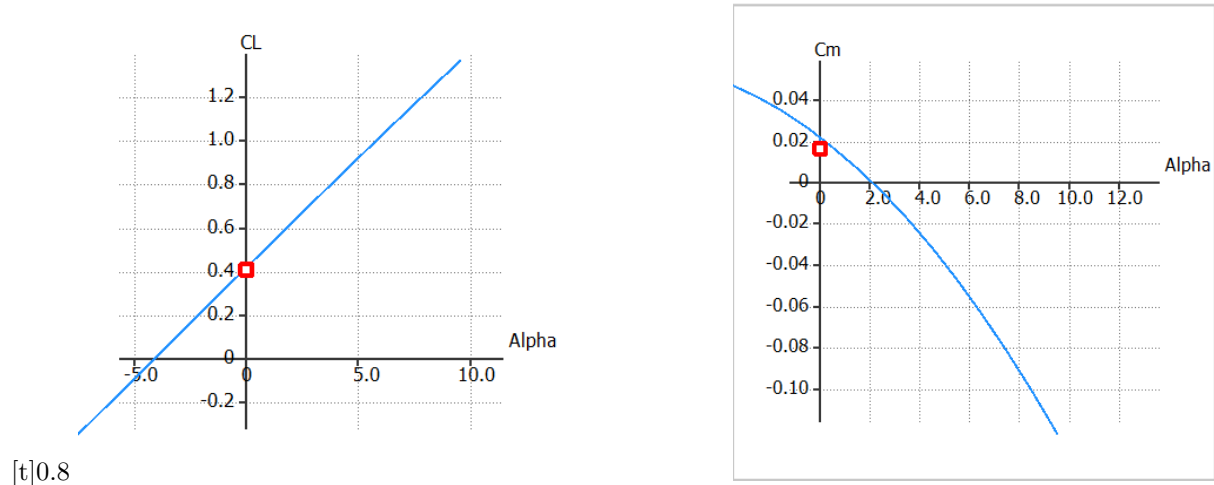


Figure 10.1.4: UAV Lift  $C_L$  and Moment  $C_M$  vs Angle of Attack  $\alpha$

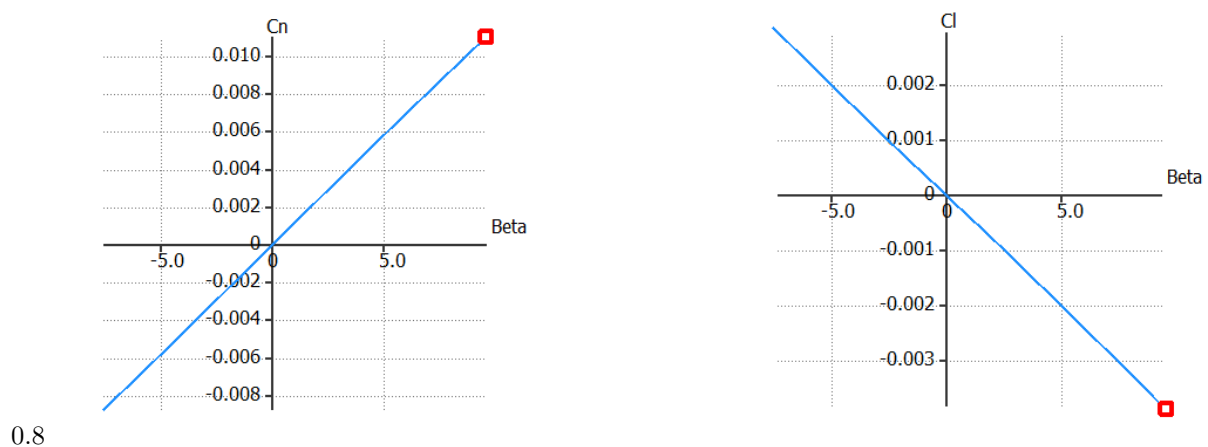


Figure 10.1.5: UAV Directional Stability  $C_n$  and Roll Stability  $C_l$  vs Sideslip angle  $\beta$

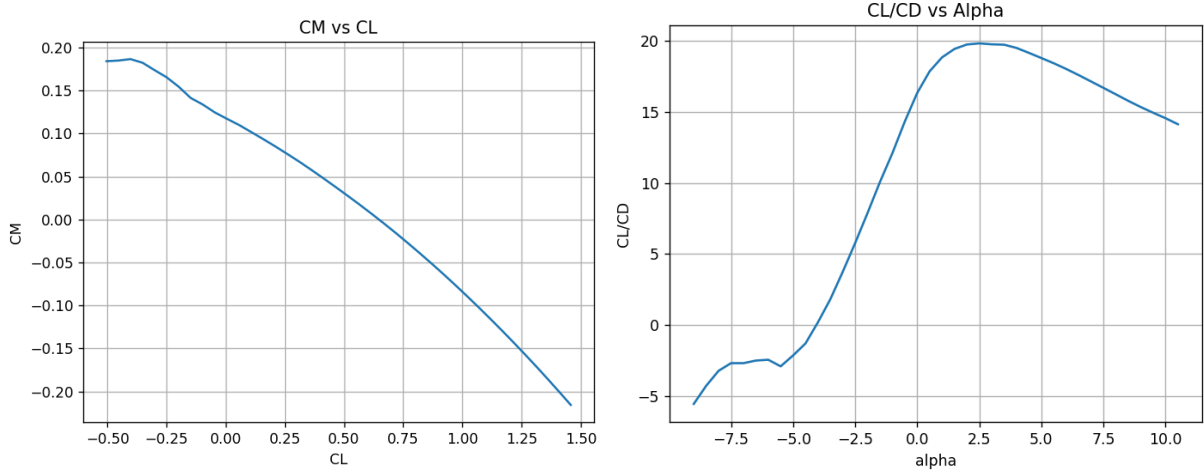


Figure 10.1.6: UAV  $C_M$  vs  $C_L$  and  $C_L/C_D$  vs Angle of Attack  $\alpha$

## 10.2 Neutral point

The neutral point ( $X_{NP}$ ) of an aircraft is the point along the chord line of the wing where the pitching moment coefficient ( $C_m$ ) remains constant, regardless of changes in the angle of attack ( $\alpha$ ). In other words, the neutral point is the point where the aircraft is neutrally stable in pitch.

The location of the neutral point is given by:

$$X_{NP} = X_{ac_w} + \eta_{ht} V_{H_{ht}} \frac{\partial C_{L_{\alpha_t}}}{\partial C_{L_{\alpha_w}}} \left( 1 - \frac{\partial \epsilon}{\partial \alpha} \right)$$

[19] Now to get the value of the position of the neutral point, CG, and aerodynamic center of the wing with respect to the leading edge of the wing along the chord line, we use simple geometry.  $X_{CG}, Z_{CG}$  are positions along FRL, and  $X'_{CG}$  is along the chord line. So we get,

$$X'_{CG} = X_{CG} \cos \theta_w - Z_{CG} \sin \theta_w \quad \text{and} \quad h_{CG} = \frac{X_{CG}}{c}$$

Here,  $\theta_w$  is the wing setting angle. Thus, using similar geometry to get  $h_{ACWB}$  and  $h_{NP}$ :

$$h_{NP} = \frac{X_{NP} \cos \theta_w - Z_{NP} \sin \theta_w}{c} \quad \text{and} \quad h_{ACWB} = \frac{X_{AC,W} \cos \theta_w - Z_{AC,W} \sin \theta_w}{c}$$

The values set for the UAV model are  $X_{AC_w} = 0.325 \text{ m}$  from the tip of the fuselage,  $\eta_{ht} = 0.8$ ,  $V_{H_{ht}} = \frac{l_t S_t}{S_w c_w} = 1.42$ , where  $S_w = 0.96 \text{ m}^2$ ,  $c_w = 0.34 \text{ m}$ ,  $l_t = 1.1 \text{ m}$ ,  $S_t = 0.42 \text{ m}^2$ , and  $\frac{d\epsilon}{d\alpha} = \frac{2C_{L_{\alpha_wing}}}{\pi AR_w} = 0.34/\text{rad}^{-1}$ .

Thus replacing the values, the  $X_{NP}$  obtained is

$$X_{NP} = 0.57 \text{ m} \tag{10.2.1}$$

[19]

## 10.3 Longitudinal Static Stability

The longitudinal stability of an aircraft is the tendency of the aircraft to return to its original pitch attitude after a disturbance. The condition for longitudinal stability is that the derivative of the pitching moment coefficient with respect to angle of attack ( $\alpha$ ) must be negative:

$$\frac{\partial C_M}{\partial \alpha} < 0 \tag{10.3.1}$$

where  $C_M$  is the pitching moment coefficient.

In other words, if the angle of attack of the aircraft is increased, the pitching moment should be such that it opposes the angle of attack change and brings the aircraft back to its original pitch attitude.

### 10.3.1 Pitching Moment Coefficient

Before calculating, it is estimated from XFLR5 that  $C_{M_{AC}} = -0.11$ ,  $C_{L_{0w}} = 0.4$ ,  $C_{L_{\alpha_w}} = 0.08/\text{°}$ ,  $C_{L_{\alpha_t}} = 0.072/\text{°}$ . We also estimate  $\frac{d\epsilon}{d\alpha} = \frac{2C_{L_{\alpha_wing}}}{\pi AR_w} = 0.34$  and  $\epsilon_o = \frac{2C_{L_{0wing}}}{\pi AR_w} = 1.73\text{°}$ . The moment coefficient at angle of attack  $\alpha = 0$  due to wing and tail is

$$C_{m_0} = C_{M_{AC_w}} + C_{L_{0w}} \left( \frac{X_{CG} - X_{AC}}{\bar{c}} \right) + \eta V_H C_{L_{\alpha_t}} (\epsilon_0 - i_t - i_w) \quad (10.3.2)$$

[28]

$$C_{m_0} = 0.048$$

Thus, the pitch moment curve slope due to the wing and tail is:

$$\frac{\partial C_m}{\partial \alpha} = C_{L_{\alpha_w}} \left( \frac{X_{CG} - X_{AC}}{\bar{c}} \right) - \eta V_H C_{L_{\alpha_t}} \left( 1 - \frac{\partial \epsilon}{\partial \alpha} \right) \quad (10.3.3)$$

[28]

$$C_{m_\alpha} = -1.089 \text{ rad}^{-1}$$

Thus, the moment polar for the UAV is (as seen in 10.1.4),

$$C_m = 0.048 - 0.019\alpha \quad (10.3.4)$$

Thus, the trim  $\alpha = 2.5\text{°}$ , which is close to the design  $\alpha(C_L/C_{Dmax}) = 2.2\text{°}$  as seen in

### 10.3.2 Static Margin

By definition, static margin refers to the distance between the neutral point and the center of gravity of the aircraft. The expression for it can be given by:

$$\text{Static Margin} = \left( \frac{X_{NP} - X_{CG}}{\bar{c}} \right) = -\frac{C_{M_\alpha}}{C_{L_\alpha}} = 0.08 \quad (10.3.5)$$

[28]

Table 10.3.1: Longitudinal Stability Parameters

Parameters	Values	Units
$X_{CG}$	0.5	m
Neutral point $X_{NP}$	0.57	m
Aerodynamic center of wing $X_{AC_w}$	0.325	m
Tail setting angle ( $i_t$ )	2.0°	deg
Absolute angle of attack at Trim	2.5°	deg
Cruise Design angle of attack	2.2°	deg
$C_m$	0.048 - 0.019α	-
Static margin	0.2	-

## 10.4 Directional Static Stability

In the context of UAV design, directional stability refers to the ability of the aircraft to maintain its intended direction of flight without excessive oscillations or deviations. This is particularly important for UAVs, which often need to fly at low altitudes and in challenging environments and require precise control for a wide range of missions.

The design of directional stability in a UAV involves the proper selection and placement of the vertical tail surfaces and other control surfaces, as well as the optimization of the aircraft's aerodynamic characteristics. One important design consideration is the yaw moment coefficient ( $C_n$ ), which represents the aircraft's tendency to yaw or turn about its vertical axis in response to changes in sideslip angle ( $\beta$ ). The condition for directional stability is typically expressed as

$$\frac{\partial C_n}{\partial \beta} > 0 \quad (10.4.1)$$

The vertical tail was adjusted in XFLR5 along with the bulk of the fuselage length to add directional stability, and the final directional slope was obtained in Fig. 5.2.3 as

$$\frac{\partial C_n}{\partial \beta} = 0.0153 \text{ rad}^{-1} \quad (10.4.2)$$

## 10.5 Lateral Stability

Lateral stability refers to the ability of an aircraft to maintain its lateral equilibrium during flight. It is a measure of the aircraft's resistance to rolling motion about its longitudinal axis and is an essential aspect of flight safety and control. Lateral stability is achieved through the proper design and placement of the aircraft's wing and other control surfaces, which generate aerodynamic forces that counteract any disturbances that may cause the aircraft to roll or bank off course.

The condition for lateral stability is typically expressed as:

$$\frac{\partial C_l}{\partial \beta} < 0 \quad (10.5.1)$$

where  $C_l$  is the rolling moment coefficient and  $\beta$  is the sideslip angle. This means that the derivative of the rolling moment coefficient with respect to sideslip angle must be negative, indicating that the aircraft generates a stabilizing rolling moment that counteracts any disturbances that may cause it to roll or bank off course.

Since the UAV is designed to survey forest cover, we take in additional considerations for the common gusts of wind and turbulent air experienced above forests, and a high wing configuration with a small roll stabilizing wing dihedral angle of  $2^\circ$  was designed. The lateral slope was obtained from XFLR5 Fig. 5.2.3:

$$\frac{\partial C_l}{\partial \beta} = -0.0076 \text{ rad}^{-1} \quad (10.5.2)$$

## 10.6 Control Surfaces

### 10.6.1 Aileron

In the design process of an aileron, four parameters need to be determined.

- Aileron platform area ( $S_a$ )
- Aileron chord/span ( $c_a/b_a$ )
- Maximum up and down aileron deflection ( $A_{max}$ )
- Location of inner edge of the aileron along the wing span ( $b_{ai}$ )

As a general guidance, the typical values for these parameters are as follows:[28]

$S_a/S = 0.05\text{--}0.1$ ,  $b_a/b = 0.2\text{--}0.3$ ,  $c_a/C = 0.15\text{--}0.25$ ,  $b_{ai}/b = 0.6\text{--}0.8$ , and  $A_{max} = \pm 30^\circ$ .

From our previous data, we use  $S = 0.95 \text{ m}^2$ ,  $b = 2.82 \text{ m}$ ,

$$\begin{aligned} S_a/S = 0.05 &\rightarrow S_a = 0.048 \text{ m}^2 \\ b_a/b = 0.2 &\rightarrow b_a = 0.564 \text{ m} \\ c_a/c = 0.25 &\rightarrow c_a = 0.085 \text{ m} \\ b_{ai}/b = 0.6 &\rightarrow b_{ai} = 1.692 \text{ m} \\ &\rightarrow A_{max} = \pm 30^\circ. \end{aligned}$$

Therefore, the factors affecting the design of the aileron are the required hinge moment, the aileron effectiveness, the aerodynamic and mass balancing, the flap geometry, the aircraft structure and the cost.

Aileron effectiveness is a measure of how effective the aileron deflection is in producing the desired rolling moment. The following image is for representation of aileron only, there is no sweep angle in our design.

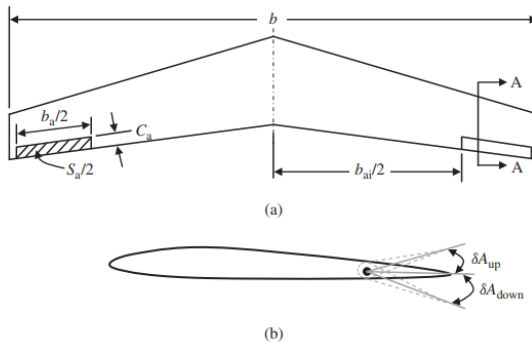


Figure 10.6.1: (a) Top view of the wing and aileron for reference ; (b) Side view of the wing and aileron for reference[28]

### 10.6.2 Elevator

The typical values of the area, span and chord of the elevator seen below are taken from the reference book [28]

$S_e/S_t : 0.15 \text{--} 0.4$

$b_e/b_t : 0.8 \text{--} 1$

$c_e/c_t : 0.2 \text{--} 0.4$

For the preliminary analysis we take the ratios to be  $S_e/S_t = 0.25$  for area,  $b_e/b_t = 1.0$  for span and  $c_e/c_t = 0.25$  for chord length and can be modified as per the requirements after doing stability analysis. Therefore, the values for the area, span and chord length for the elevator comes out to be

$S_e : 0.105 \text{ m}^2$

$b_e : 1.5 \text{ m}$

$c_e : 0.07 \text{ m}$

### 10.6.3 Rudder

The typical values of the area, span and chord of the Rudder seen below are taken from the reference book [28]

$$S_r/S_v : 0.150.35$$

$$b_r/b_v : 0.71$$

$$c_r/c_v : 0.150.4$$

For the preliminary analysis we take the ratios to be  $S_r/S_v = 0.3$  for area,  
 $b_r/b_v = 0.8$  for span and  
 $c_r/c_v = 0.3$  for chord length

These values can be modified as per the requirements after doing stability analysis. Therefore, the values for the area, span and chord length for the rudder comes out to be

$$S_r = 0.042m^2$$

$$b_r = 0.4m$$

$$c_r = 0.105m$$

## 10.7 Flight Controller

In order to maintain a safe flight profile with sufficient maneuverability and control-ability, the UAV needs to be equipped with a flight controller. Considering our design parameters, flight control dimensions and flight profile we have selected the Ublox NEO-7M Flight Controller with GPS module. The flight controller comes with an onboard GPS which provides an added advantage for accurate navigation. The main features of the Flight Controller Module are as listed below:-

- Ublox Neo 7M GPS module includes an HMC5883L digital compass.
- Ublox NEO 7 series is a high-sensitivity, low-power GPS module that has 56 channels and outputs precise position. The GPS module also comes with a moulded plastic case which keeps the module protected against the environmental elements making it ideal for use on UAVs
- The NEO-7 series provides maximum sensitivity while maintaining low system power.
- RF integration. Sophisticated RF architecture and interference suppression ensure maximum performance even in GPS-hostile environments.

# Chapter 11

## Performance Calculation

### 11.1 Drag Polar

#### 11.1.1 $S_{wet}$

The calculation of drag requires the wetted and the reference. The wetted areas for different components are calculated from the three-point view and the CAD model of our UAV. The reference area ( $S_{ref}$ ) is the projected area (platform area) of the wing. The wetted area for the wing, horizontal and vertical tail is approximately twice the platform area. All the values of  $S_{wet}$  and  $S$  are tabulated in the following table:

Component	Area (m <sup>2</sup> )	
	$S_{ref}$	$S_{wet}$
Fuselage	0.27	1.7
Wing	0.96	1.96
Horizontal tail	0.39	0.67
Vertical tail	0.13	0.17

Table 11.1.1: Area of components (m<sup>2</sup>)

#### 11.1.2 $C_{D_o}$ Calculation

We need the value of  $C_{D_o}$  to plot the drag variation for our specific UAV based on the parameters we have calculated. The following formulae are used with same assumptions as previously stated during the T/W calculations 13.2. The final aspect ratio(AR) chosen is 8.3 and Reynolds number is 411400.

$$C_{D_o} = \frac{C_f \cdot S_{wet}}{S_{ref}} = 0.03 \quad (11.1.1)$$

[28]

$$C_f = \frac{0.074}{Re^{1/7}} = 0.0116 \quad (11.1.2)$$

[28]

$$e = \frac{1}{1.05 + 0.007 \cdot \pi AR} = 0.8113 \quad (11.1.3)$$

[28]

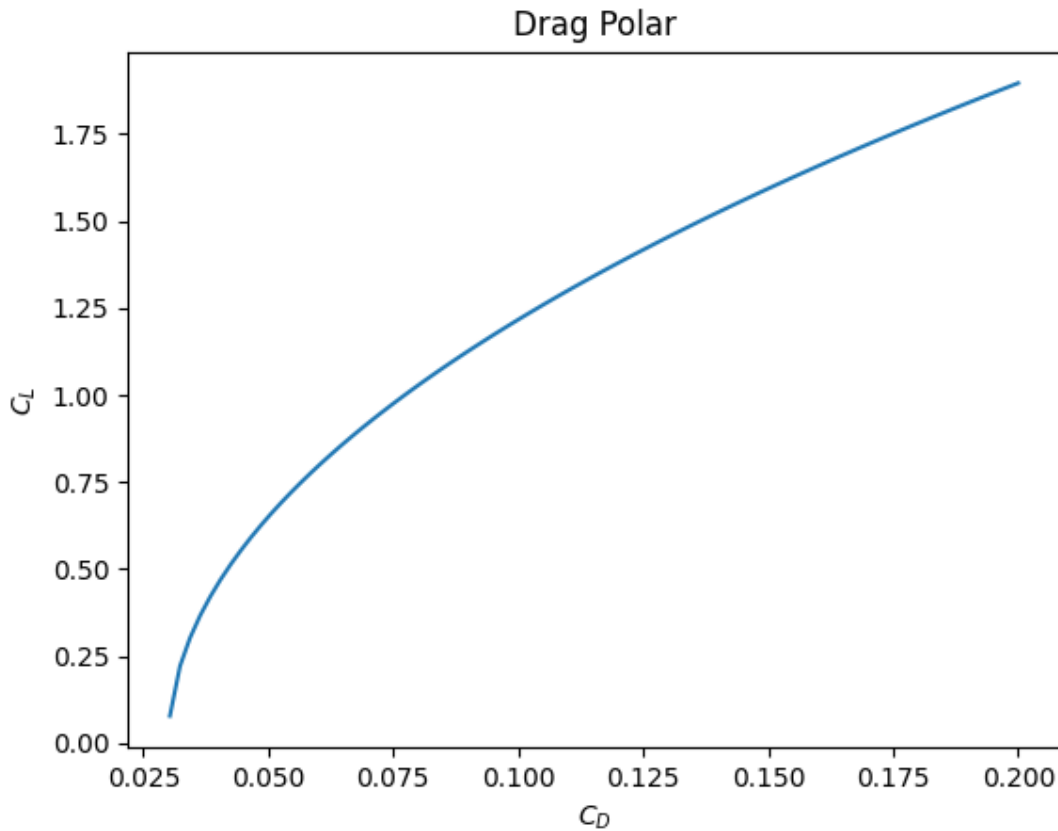


Figure 11.1.1: Drag Polar

$$C_D = C_{D_0} + \frac{1}{\pi e AR} C_L^2 \quad (11.1.4)$$

[28]

## 11.2 Final Power Estimates

After simulating and adjusting the UAV's design, and conceptually creating it in a CAD software, the Power estimation process is revisited to investigate the performance of the UAV. The final mass of the CAD Model of the UAV is estimated at 9kg. The pre-determined  $C_L$  values according to which the UAV was designed are again stated here to facilitate final estimates of the required power for each significant phase of flight.

$C_L$	Values
$C_{L_{cruise}}$	0.5
$C_{L_{stall}}$	1.42
$C_{L_{takeoff}}$	1.21
$C_{L_{climb}}$	1.31

### 11.2.1 Takeoff

The power required for Takeoff is estimated as

$$P_{takeoff} = \frac{1}{2} \rho v_{takeoff}^3 C_{D_{takeoff}} \quad (11.2.1)$$

Where  $AR = 8.3$ ,  $e = 0.81$ ,  $\rho_{ground} = 1.225 \text{ kg/m}^3$ ,  $v_{takeoff} = 11 \text{ m/s}$   
 $\phi = \frac{(16h/b)^2}{1+(16h/b)^2} = 0.71$  as ground clearance  $h = 0.275 \text{ m}$  and wing span  $b = 2.82 \text{ m}$

Thus, Drag Coefficient for take off  $C_{D_{takeoff}} = C_{D_o} + \phi \frac{1}{\pi e AR} C_{L_{takeoff}}^2 = 0.08$   
 Which can be finally substituted to get

$$P_{takeoff} = 65 \text{Watt} \quad (11.2.2)$$

### 11.2.2 Climb

The power required for Climbing Flight is estimated as

$$P_{climb} = T_{climb}v_{climb} = \frac{1}{2}\rho v_{climb}^3 SC_D + Wv_{climb} \sin\gamma \quad (11.2.3)$$

Where  $AR = 8.3$ ,  $e = 0.81$ ,  $\rho = 1.225 \text{kg/m}^3$

Climb Rate = 2 m/s, Pitch Angle = 9°,  $v_{climb} = \frac{2}{\sin(9^\circ)} = 13 \text{m/s}$

Thus, Drag Coefficient for climbing flight  $C_{D_{climb}} = C_{D_o} + \frac{1}{\pi e AR} C_{L_{climb}}^2 = 0.111$

Which can be finally substituted to get

$$P_{climb} = 276 \text{Watt} \quad (11.2.4)$$

### 11.2.3 Cruise

The power required during the cruise phase of flight at 100 m can be estimated as

$$P_{cruise} = T_{cruise}v_{cruise} = \frac{1}{2}\rho_{100 \text{m}} v_{cruise}^3 S_{wing} C_D \quad (11.2.5)$$

Where  $\rho_{100 \text{m}} = 1.21 \text{kg/m}^3$ ,  $v_{cruise} = 18 \text{m/s}$ ,  $S_{wing} = 0.96 \text{m}^2$

Thus, the drag coefficient for cruise flight  $C_{D_{cruise}} = C_{D_o} + \frac{1}{\pi e AR} C_{L_{cruise}}^2 = 0.042$

Which can be finally substituted to get

$$P_{cruise} = 142 \text{Watt} \quad (11.2.6)$$

$P_{Power_{phase}}$	$T_{phase}$
$P_{takeoff}$	10 s
$P_{climb}$	5 min
$P_{cruise}$	1 hour

## 11.3 Range and Endurance

The maximum Discharge Rate (C) of our battery [17] is 30C and the rated voltage is 22.6V. We need to make sure that we for the power requirement for each phase the battery does not get discharged completely.

$$Time = \frac{Voltage(V) \cdot BatteryCapacity(Ah)}{Power(W)} \quad (11.3.1)$$

Using this for each phase power requirements, we find that the endurance would ideally be more than **1.5 hours** due to climb and takeoff being short duration phases.

$$Range = Endurance \cdot v_{cruise} \quad (11.3.2)$$

Hence, the range would ideally be close to **97.2 km**.

## 11.4 V - n Diagram

Every possible combination of speeds, altitudes, and configurations is included in an aircraft's flight regime. The aircraft's dynamics, aerodynamics, propulsion, and structure all influence this regime. The terms "flight envelope" and "manoeuvring envelope" refer to the boundaries of this flight regime. Pilots are constantly instructed not to fly outside of the flight envelope because the aircraft is not stable, controllable, or physically strong enough outside of certain parameters. If an aircraft is flown outside of its

flight envelope, an accident or crash is predicted.

The V-n diagram is the most important flight envelope involved in preliminary design. It helps in visualising the loads on the aircraft and determines the limits on maneuvering based on the maximum loads the aircraft. The critical points of the diagram are calculated as below.

The load factor  $n$  is defined as:

$$n = \frac{L}{W} = \frac{1}{2} \frac{\rho v^2 S C_{L_{max}}}{W} \quad (11.4.1)$$

Typically, the maximum and minimum values of load factor are 3 and -1 respectively. The following V-n diagram of our aircraft shows the conditions of the stall - positive and negative stall curve, maximum and minimum structural limit, and maximum allowable velocity.

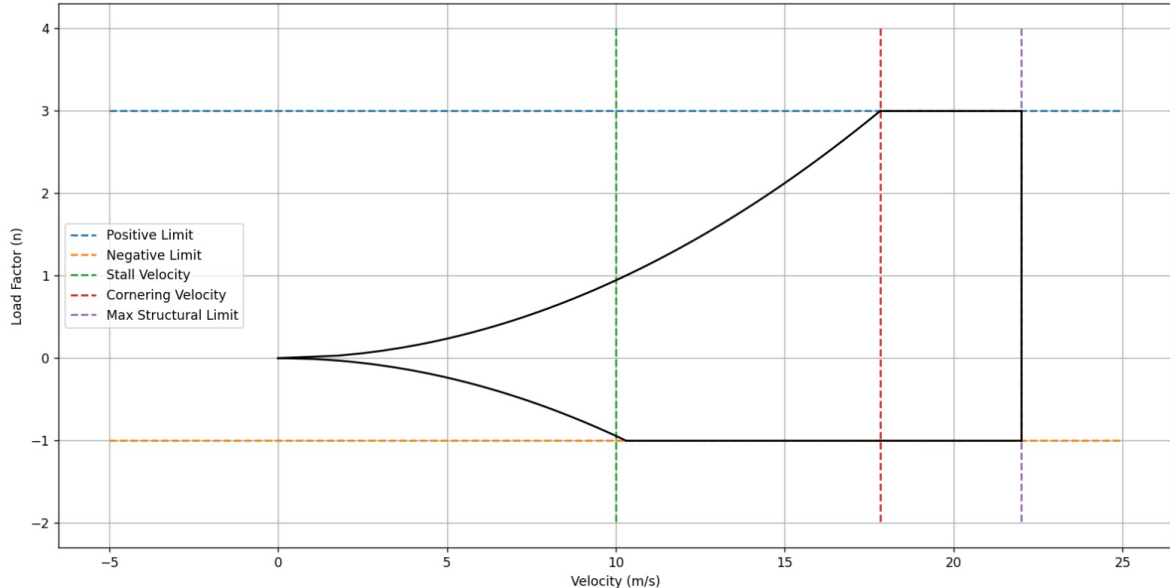


Figure 11.4.1: V - n diagram

- The maximum load factors that an aeroplane may safely handle without experiencing structural failure is known as the **structural limit**.
- **Cornering velocity** is 5.4 m/s.
- **Lift Limit** is the highest load factor that may be achieved at a specific speed; if exceeded, a stall might happen.
- **Diving Speed** assists in determining the highest safe diving speed in order to prevent going above structural limitations.
- **Dynamic Pressure** concerns the maximum aerodynamic forces an aeroplane encounters at a given speed.
- **Safety Margin** specifies the operating bounds that an aircraft can fly inside without risk.

To ensure a conservative and safe design, it is generally recommended to choose load factors towards the lower end of the range. This provides a greater margin of safety and helps account for uncertainties in operational conditions and potential load variations.

## Chapter 12

# Final Summary

Parameter	Value
Cruise Speed	18 m/s
Max Speed	22.5 m/s
Stall Speed	10 m/s
Rotation Speed	11 m/s
Take off Speed	12 m/s
Climb Speed	11.51 m/s
Max Climb Rate	2 m/s
Max Climb Angle	12 Deg
Absolute Ceiling	100m
Cruise Altitude	80m/40m
Propeller Efficiency	0.5
L/D	19.48
Battery Capacity	18000 mAH
Tail arm	1.2 m

Table 12.0.1: General UAV Specifications

Parameters	Value
Wing Area	0.96 $m^2$
Wing Span	2.82 m
Taper Ratio	1
Root Chord	0.34 m
Tip Chord	0.34 m
Aspect Ratio	8.3
Twist Angle	0 Deg
Sweep Angle	0 Deg
Dihedral Angle	2 Deg
Wing Setting Angle	1 Deg
Aerofoil	GOE 553
Alieron Area	0.048 $m^2$
Alieron Chord	0.085 m
Alieron Span	0.564 m

Table 12.0.2: Wing Specifications

Parameters	Value
Tail Area	$0.42 \text{ m}^2$
Tail Span	1.5 m
Taper Ratio	1
Root Chord	0.28 m
Tip Chord	0.28 m
Aspect Ratio	5.0
Twist Angle	0 Deg
Sweep Angle	0 Deg
Dihedral Angle	0 Deg
Tail Setting Angle	2 Deg
Aerofoil	NACA 0014
Elevator Area	$0.105 \text{ m}^2$
Elevator Chord	0.07 m
Elevator Span	1.5 m

Table 12.0.3: Horizontal Tail Specifications

Parameters	Value
Tail Area	$0.14 \text{ m}^2$
Tail Span	0.4 m
Taper Ratio	1
Root Chord	0.35 m
Tip Chord	0.35 m
Aspect Ratio	1.14
Twist Angle	0 Deg
Sweep Angle	0 Deg
Dihedral Angle	0 Deg
Tail Setting Angle	0 Deg
Aerofoil	NACA 0014
Rudder Area	$0.042 \text{ m}^2$
Rudder Chord	0.105 m
Rudder Span	0.4 m

Table 12.0.4: Vertical Tail Specifications

Parameter	Value
Length	1.2 m
Diameter	0.250 m
Width	0.2m
Radial Tolerance	5.00 %
Axial Tolerance	10.00 %
Radial Tolerance	5.00 %
Axial Tolerance	10.00 %

Table 12.0.5: Fuselage Specifications

Parameters	Value
MTOW	9.85 Kg
Max Payload Weight	2.0 Kg
Design Payload Weight	1.5 Kg
Powerplant Weight	2.27 Kg
CG location (from nose)	0.5 m

Table 12.0.6: Weights

Parameters	Value
$C_{L_{max}}$	1.56
$C_{L_{TakeOff}}$	1.21
$C_{L_{Stall}}$	1.42
$C_{L_{Climb}}$	1.31
$C_{L_{Cruise}}$	0.46
Oswalds Efficiency factor	0.8113
$C_{D_0}$	0.03
Wing Loading	90 N/ $m^2$

Table 12.0.7: Aerodynamic Characteristics

# Chapter 13

## Appendix

### 13.1 First Weight and Power Estimate Calculation

```
import numpy as np
import matplotlib.pyplot as plt
import math

# Data Collection
#Wo = np.array([13.5, 10.0, 6.8, 16.5, 24, 2.5])
Wo = np.array([13.5, 16.5, 6.8, 24, 2.5]) # List of all Full Weight for collected UAV data
#We_Wo = np.array([0.58, 0.44, 0.48, 0.54, 0.34, 0.84])
We_Wo = np.array([0.6, 0.7, 0.55, 0.34, 0.84]) # List of all Empty Weight Ratios for
    collected UAV data
cols = len(Wo)

#Regression Curve Fitting
x = np.column_stack((np.log(Wo), np.ones(cols)))
y = np.log(We_Wo)
B = np.linalg.lstsq(x, y, rcond=None)[0]
L = B[0]
A = math.e**B[1]
print(f'L = {L}, A = {A}')
MSE = (1/cols)*np.sum((np.square(np.subtract(We_Wo,A*Wo**L))))
print(f'MSE = {MSE}')

Wo_x = np.array([0.1*i for i in range(10, 300)])
We_Wo_y = A*Wo_x**L

# Iteration
W_pay = 2 # kg
W_batt = 2 # kg
Woi = 8 #initial total weight guess
We_Wo_est = [1 - W_batt/Woi - W_pay/Woi]
Wo_est = [W_pay/(1 - W_batt/Woi - We_Wo_est[0])]

print(f'Initial W_o = {Wo_est[0]}, Initial W_e/W_o = {We_Wo_est[0]}')
j = 0
for i in range(0,50):
    We_Wo_est_i = A*Wo_est[-1]**L
    #Wo_est_i = (W_pay/(1 - (W_batt/Wo_est[-1]) - We_Wo_est_i))
    Wo_est_i = ((W_pay+W_batt)/(1 - We_Wo_est_i))
    print(f'Iteration {i+1}')
    print(f'W_o = {Wo_est_i} kg, Empty Weight Fraction = {We_Wo_est_i}, Battery Weight
        Fraction = {W_batt/Wo_est[-1]}')
    if not math.isnan(We_Wo_est_i) and not math.isnan(Wo_est_i) and (Wo_est_i > 0):
        We_Wo_est.append(We_Wo_est_i)
        Wo_est.append(Wo_est_i)
```

```

        j = j+1
    else:
        print(We_Wo_est_i)
        print(Wo_est_i)
        #break

print(f"Final Estimation: W_o = {Wo_est[-1]} kg, Empty Weight Fraction = {We_Wo_est[-1]}")

plt.figure(1,dpi=100)
plt.plot(np.log(Wo_x), np.log(We_Wo_y))
plt.scatter(np.log(Wo), np.log(We_Wo))
plt.scatter(np.log(Wo_est), np.log(We_Wo_est))
plt.xlabel("log($W_o$)")
plt.ylabel("log($W_e/W_o$)")
plt.show()

plt.figure(1,dpi=100)
plt.plot(Wo_x, We_Wo_y)
plt.scatter(Wo, We_Wo)
#plt.scatter(Wo_est, We_Wo_est)
plt.xlabel("$W_o$")
plt.ylabel("$W_e/W_o$")
plt.show()

plt.figure(1,dpi=100)
plt.plot([i for i in range(0,30)], Wo_est[:30])
plt.xlabel("No of iterations")
plt.ylabel("Final Weight $W_o$ (kg)")
plt.show()

# Power Calculation
AR = 8.89 # Initial Aspect Ratio Estimate
S = 0.76 # m^2, Initial Wing Surface Area Estimate
h = 0.050 #ground clearance
b = 2 #wingspan
phi = (((16*h)/b)**2)/(1+((16*h)/b)**2)#ground effect

CLmax = 0.8
CD0 = 0.03 # Initial CD,0 Estimate
e = 0.8 #oswald efficiency

rho = 1.225 #kg/m^3, Sea Level Density
g = 9.81 # m/s^2, Acceleration due to gravity
mass = Wo_est[-1] # kg, First Weight estimate
W = Wo_est[-1]*g # N

angle_of_climb = 10*math.pi/180 # Initial Angle of Climb estimate of 10 deg
V_cruise = 18 #m/s, Initial Cruise Velocity Estimate
V_climb = 2/(math.sin(angle_of_climb)) #m/s, Initial Climb Velocity Estimate
V_stall = math.sqrt((2*W)/(rho*S*CLmax))
V_takeoff = 1.3*V_stall

Voltage = 9 # V, Battery Power Supply

CD_cruise = CD0 + (1/(math.pi*e*AR))*(W/(0.5*rho*(V_cruise**2)*S))**2
CD_climb = CD0 + (1/(math.pi*e*AR))*(W/(0.5*rho*(V_climb**2)*S))**2
CD_takeoff = CD0 + phi*(1/(math.pi*e*AR))*(W/(0.5*rho*(V_takeoff**2)*S))**2

P_cruise = 0.5*rho*(V_cruise**3)*S*CD_cruise
P_climb = 0.5*rho*(V_climb**3)*S*CD_climb + W*math.sin(angle_of_climb)*V_climb
P_takeoff = 0.5*rho*(V_takeoff**3)*S*CD_takeoff

T_takeoff = 10/(60*60)

```

```
T_climb = 5/60
T_cruise = 1
sf=1;

mAh = sf*(P_takeoff*T_takeoff+P_climb*T_climb+P_cruise*T_cruise)*1000/Voltage
print(f"P_cruise = {P_cruise} W, P_climb = {P_climb} W, P_takeoff = {P_takeoff} W")
print(f"Total Watt Hour = {P_takeoff*T_takeoff+P_climb*T_climb+P_cruise*T_cruise} Wh, {mAh}
      mAh Battery, {Voltage} Voltage")
```

---

## 13.2 T/W Calculation

```
import numpy as np
import matplotlib.pyplot as plt
import math

rho = 1.21; #approximate density at height range 50-100m
eta = 0.000018; #approximate coefficient of viscosity at height range 50-100m
c = np.array([0.136,0.22,0.0543]); #list of chord length
v = np.array([18.88,17,20]) #30,16.67,16,16,20]; #cruise speed of UAV
Re = rho*c*v/eta
print("Reynolds Number = ",Re)
Cf = 0.074/(np.power(Re,(1/7)))
print("Skin friction coefficient = ",Cf)

k = 1;#k is a constant that depends on the aircraft configuration and Reynolds number.
Swet = np.array([1.2206,0.50549,0.845]);#wetted area of aircraft
Sref = np.array([0.9248,0.39257,0.555]);#reference area of aircraft
Cdo = k*Cf*(Swet/Sref);#zero lift drag
print("Cdo = ",Cdo)

AR = np.array([13.6,12.32,11.255]); #list of aspect ratios of all UAVs
eo = 0.8; #efficiency factor of wing planform
e = 1/(1.05+0.007*math.pi*AR); #Oswald efficiency
twmin = np.sqrt((4*Cdo)/(math.pi*e*AR)); #calculation of T/W min
twmin = np.append(twmin,np.array([1/20.6875,1/14,1/26,1/19.05]))
L_D = 1/twmin;
print("(L/D)_max = ",L_D)
print("(T/W)_min = ",twmin)
print("Oswald Efficiency: ",e)

v=np.append(v,np.array([16,16,20,30]));
print("v_cruise = ",v);
AR=np.append(AR,np.array([4,6,8.89,5.55]))


cols = len(L_D)
x = np.column_stack((np.log(v), np.ones(cols)))
y = np.log(L_D)
B = np.linalg.lstsq(x, y, rcond=None)[0]
L = B[0]
A = math.e**B[1]
#print(f'L = {L}, A = {A}')
MSE = (1/6)*np.sum((np.square(np.subtract(L_D,A*v**L))))
#print(f'MSE = {MSE}')

V_plot = np.array([0.1*i for i in range(1,500)])
L_D_plot = A*V_plot**L
print(f'Design L/D = {A*17**L} to {A*19**L}')
#L/D vs v_cruise
plt.figure(1, dpi = 100)
plt.plot(V_plot, L_D_plot)
plt.plot([18 for i in range(8,30)], [i for i in range(8,30)])
plt.scatter(v, L_D)
plt.scatter([17,19], [A*17**L, A*19**L])
plt.xlabel("V_Cruise")
plt.ylabel("L/D Max")
plt.show()
ldmax=A*18**L
print("L/D max plot= ",ldmax)
print("T/W min plot= ",1/ldmax)
```

```

x = np.column_stack((np.log(AR), np.ones(cols)))
y = np.log(L_D)
B = np.linalg.lstsq(x, y, rcond=None)[0]
L_ar = B[0]
A_ar = math.e**B[1]
#print(f"L = {L_ar}, A = {A_ar}")
MSE = (1/6)*np.sum((np.square(np.subtract(L_D,A*AR**L))))
#print(f"MSE = {MSE}")

AR_plot = np.array([0.1*i for i in range(1,500)])
L_D_plot = A*AR_plot**L
#L/D vs AR
plt.figure(1, dpi = 100)
plt.plot(np.sqrt(AR_plot), L_D_plot)
plt.plot([i for i in range(0,10)],[19 for i in range(0,10)])
plt.scatter(np.sqrt(AR), L_D)
plt.xlabel("AR")
plt.ylabel("L/D Max")
plt.show()
print("AR plot: ", (1/L)*math.log(ldmax/A))

pw=np.multiply(np.cos(7*math.pi/180)*twmin,v)

# Power Calculation
S = 4 # m^2, Initial Wing Surface Area Estimate
CLmax = 0.8
CD0 = 0.03 # Initial CD,0 Estimate
e = 0.8 #oswald efficiency

rho = 1.225 #kg/m^3, Sea Level Density
g = 9.81 # m/s^2, Acceleration due to gravity
W = 9.61*g # N

angle_of_climb = 5*math.pi/180 # Initial Angle of Climb estimate of 10 deg
V_cruise = 18 #m/s, Initial Cruise Velocity Estimate
V_climb = 2/(math.sin(angle_of_climb)) #m/s, Initial Climb Velocity Estimate
V_stall = math.sqrt((2*W)/(rho*S*CLmax))
V_takeoff = 1.3*V_stall

tw=max(twmin)
P_cruise = tw*W*V_cruise
P_climb = tw*0.5*rho*S*CLmax*V_climb**3 + W*math.sin(angle_of_climb)*V_climb
P_takeoff = tw*W*V_takeoff

print(f"P_cruise = {P_cruise} W, P_climb = {P_climb} W, P_takeoff = {P_takeoff} W")

```

---

### 13.3 W/S Calculation for Multiple Phases of Flight

```
Estimation of W/S
% Define the function for W_P in terms of W_S
W_P = @(W_S) (1 - exp((2.8264 / W_S))) / ...
(0.03 - (0.03 + 2.925 / W_S) * exp((2.8264 / W_S))) * 0.04167;

% Define the target value of W/P
target_W_P = 0.0177;

% Define an anonymous function for the difference between the target and actual W/P
diff_W_P = @(W_S) abs(W_P(W_S) - target_W_P);

% Find the value of W/S that minimizes the difference
W_S_solution = fminsearch(diff_W_P, 1); % Start with an initial guess of 1 for W_S

% Calculate the corresponding W/S value
W_S = W_S_solution;
W = 0.0177 * W_S;

disp(['The value of W/S at W/P = 0.0177 is: ', num2str(W_S)]);
disp(['The corresponding value of W is: ', num2str(W)]);

For graph
% Generate W/S values
W_S_range = linspace(1, 50, 100); % Adjust range as needed

% Calculate W/P for each W/S
W_P = (1 - exp((2.8264 ./ W_S_range))) ./ (0.03 - (0.03 + 2.925 ./ W_S_range) .* ...
exp((2.8264 ./ W_S_range))) .* 0.04167;

% Create the plot
figure;
plot(W_S_range, W_P, 'b-'); % Blue line
xlabel('W/S (Wing loading)');
ylabel('W/P (Power loading)');
title('W/P vs W/S');
grid on; % Add grid lines for better readability
```

---

```
import numpy as np
import matplotlib.pyplot as plt
import math

rho = 1.225
S = 0.9
CDo = 0.04
e_ = 0.8
AR = 9
m = 7.8
g = 9.81
W = m*g
K = 1/(math.pi*e_*AR)
n_prop = 0.8
L__D_max = 19.48
# CDo = 1/(4*K)*(1/L__D_max)**2
# L__D_max = math.sqrt(CDo/K)/(2*CDo)
CLmax = L__D_max*2*CDo
print(f"L/D max = {L__D_max}")
print(f"CDo = {CDo}, L__D_max = {L__D_max}, CL_max = {CLmax}")
```

```

# Stall Speed
V_stall = 10
W_S_stall = 0.5*rho*V_stall**2*S*CLmax
print(W_S_stall)
W_S_stall = np.ones(7)*W_S_stall
W_P = np.array([0.1*i for i in range(0,7)])

# Cruise Speed or Max Speed
V_max = 18
# CD = CDo + K*(2*W/(rho*V_max**2*S))**2
W_S = np.array([0.1*i for i in range(1,1000)])
W_P_s1 = n_prop/(0.5*rho*V_max**3*CDo/W_S + 2*K*W_S/(rho*V_max**2))

# Take Off Run
V_TO = V_stall*1.2
nu = 0.03 # Friction Coeff
CLto = 0.8*CLmax
CDto = CDo + 0.009 + 0.005 + K*CLto**2
CDg = CDto - nu*CLto
Vr = 1.2*V_stall
Sto = 100
CLR = 2*W/(1.225*0.8*Vr**2)
W_P_TO = (1-np.exp(0.6*rho*g*CDg*Sto*1/W_S))/(0.04 -
(0.04+CDg/CLR)*(np.exp(0.6*rho*g*CDg*Sto*1/W_S)))*0.5/V_TO

# ROC
ROC = 2
W_P_ROC = 1/(ROC/0.5+1.155/(L_D_max*0.5)*np.sqrt(2*W_S/(rho*math.sqrt(3*CDo/K))))


plt.figure(1, dpi = 100)
plt.plot(W_S_stall/g, W_P)
plt.plot(W_S/g, W_P_s1)
plt.plot(W_S/g, W_P_TO)
plt.plot(W_S/g, W_P_ROC)
plt.xlabel("W/S WING LOADING (kg/m^2)")
plt.ylabel("W/P POWER LOADING (N/Watt)")
plt.legend(["Stall Speed", "Cruise Velocity", "Take Off Run", f"Rate of Climb = {ROC} m/s"])
plt.show()

```

---

## 13.4 Second Weight Estimate Calculation

```
import numpy as np
import matplotlib.pyplot as plt
import math

# Data Collection
Wo = np.array([13.5, 10.0, 6.8, 16.5, 24, 2.5]) # List of all Full Weight for collected UAV
    data
We_Wo = np.array([0.58, 0.44, 0.48, 0.54, 0.34, 0.84]) # List of all Empty Weight Ratios
    for collected UAV data
Wb_Wo = np.array([0.34, 0.24, 0.37, 0.28, 0.43, 0.2]) # List of all EBattery Weight Ratios
    for collected UAV data
cols = len(Wo)

# Regression Curve Fitting
x = np.column_stack((np.log(Wo), np.ones(cols)))
y = np.log(We_Wo)
B = np.linalg.lstsq(x, y, rcond=None)[0]
L = B[0]
A = math.e**B[1]
print(f'L = {L}, A = {A}')
MSE = (1/cols)*np.sum((np.square(np.subtract(We_Wo,A*Wo**L))))
print(f'MSE = {MSE}')

Wo_x = np.array([0.1*i for i in range(10, 300)])
We_Wo_y = A*Wo_x**L

# Iteration
W_pay = 2.0 # kg
W_batt = 1.5 # kg
W_motor = 550/1000 #kg
W_prop = 54.2/1000 #kg
W_pp = W_batt + W_prop + W_motor ; #kg
We_Wo_est = [0.5]
Wo_est = [(W_pay + W_pp)/(1 - We_Wo_est[0])]
print(f'Initial W_o = {Wo_est[0]}, Initial W_e/W_o = {We_Wo_est[0]}')
j = 0
for i in range(0,40):
    We_Wo_est_i = A*Wo_est[i]**L
    print(f'Iteration {i}')
    print(f'W_o = {Wo_est[i]} kg, Empty Weight Fraction = {We_Wo_est[i]}, Powerplant Weight
        Fraction = {W_pp/Wo_est[i]}')
    # print(f'Battery Ratio : {W_batt/Wo_est[i]}')
    Wo_est_i = (W_pay + W_pp)/(1 - We_Wo_est_i)
    if not math.isnan(We_Wo_est_i) and not math.isnan(Wo_est_i) and (Wo_est_i > 0):
        We_Wo_est.append(We_Wo_est_i)
        Wo_est.append(Wo_est_i)
        j = j+1
    else:
        break
print(f'Final Estimation: W_o = {Wo_est[-1]} kg, Empty Weight Fraction = {We_Wo_est[-1]}')

plt.figure(1,dpi=100)
plt.plot(np.log(Wo_x), np.log(We_Wo_y))
plt.scatter(np.log(Wo), np.log(We_Wo))
plt.scatter(np.log(Wo_est), np.log(We_Wo_est))
plt.xlabel("log(W_o)")
plt.ylabel("log(W_e/W_o)")
plt.show()

plt.figure(1,dpi=100)
```

```
plt.plot(Wo_x, We_Wo_y)
plt.scatter(Wo, We_Wo)
plt.scatter(Wo_est, We_Wo_est)
plt.xlabel("W_o")
plt.ylabel("W_e/W_o")
plt.show()

plt.figure(1,dpi=100)
plt.plot([i for i in range(0,j+1)], Wo_est)
plt.xlabel("No of iterations")
plt.ylabel("Final Weight W_o (kg)")
plt.show()
```

---

## 13.5 Fuselage Length Estimation

---

```
import numpy as np
import matplotlib.pyplot as plt
from scipy.optimize import curve_fit

# Define the power law function
def power_law(W, a, c):
    return a * np.power(W, c)

# Example data (replace this with your actual data)
weights = np.array([35,20,13.5,7.8]) # W
lengths = np.array([2.8,2.06,1.26,1.3]) # L

# Fit the power law curve to the data
popt, pcov = curve_fit(power_law, weights, lengths)

# Extract the fitted parameters
a_fit, c_fit = popt

# Print the fitted parameters
print("Fitted parameter a:", a_fit)
print("Fitted parameter c:", c_fit)

# Generate points on the fitted curve for plotting
weights_curve = np.linspace(min(weights), max(weights), 100)
lengths_curve = power_law(weights_curve, a_fit, c_fit)

# Plot the data points and the fitted curve
plt.figure(figsize=(8, 6))
plt.scatter(weights, lengths, label='Data Points')
plt.plot(weights_curve, lengths_curve, label='Fitted Power Law Curve', color='red')
plt.xlabel('Weight ($W_0$)')
plt.ylabel('Length (L)')
plt.title('Power Law Fit: L = a$W_0^{c}$')
plt.legend()

# Choose a point on the curve
chosen_weight = 8.8
chosen_index = np.where(weights_curve < chosen_weight)[-1][-1]
chosen_length = lengths_curve[chosen_index]
plt.scatter(chosen_weight, chosen_length, color='green', label='Chosen Point on Curve')
plt.annotate(f'({chosen_weight:.2f}, {chosen_length:.2f})', (chosen_weight, chosen_length),
            textcoords="offset points", xytext=(5,5), ha='center')
plt.legend()

plt.grid(True)
plt.show()
```

---

## 13.6 Conceptual Horizontal Tail Area Sizing Calculation

---

```
import numpy as np
import matplotlib.pyplot as plt

alpha = np.linspace(-7, 13, 100)
CM_w = -0.2-0.02*alpha

n = 0.9
CL_a = 0.08
i_w = 1
i_t = -3
e_o = 1.73
de_da = 0.34

V_H = np.array([0.4, 0.5, 0.6, 0.7, 0.8, 0.9, 1.0, 1.1, 1.2, 1.3])
S_w = 0.96
l_t = 1.159
c_w = 0.34
S_t = V_H*S_w*c_w/l_t
CM_Total = []
print(S_t)
for v_h in V_H:
    CM_t = n*v_h*CL_a*(i_w+e_o-i_t) - n*v_h*CL_a*alpha*(1-de_da)
    CM_total = CM_w + CM_t
    CM_Total.append(CM_total)
    # plt.figure()
    # plt.plot(alpha, CM_total)
    # plt.plot(alpha, CM_w)
    # plt.xlim([0,13])
    # plt.legend(["total", "wing"])
    # plt.show()

plt.figure()
plt.plot(alpha, CM_w)
for cm in CM_Total:
    plt.plot(alpha, cm)
plt.xlim([0,13])
plt.legend(["only wing", "V_H = 0.4, St = 0.114m^2", "V_H = 0.5, St = 0.144m^2", "V_H = 0.6, St = 0.172m^2", "V_H = 0.7, St = 0.2m^2",
           "V_H = 0.8, St = 0.23m^2", "V_H = 0.9, St = 0.258m^2", "V_H = 1.0, St = 0.287m^2", "V_H = 1.1, St = 0.316m^2",
           "V_H = 1.2, St = 0.344m^2", "V_H = 1.3, St = 0.373m^2"])
plt.xlabel("alpha")
plt.ylabel("CM_total")
plt.show()
```

---

## 13.7 Drag Polar Calculation

```
import numpy as np
import matplotlib.pyplot as plt

# Define parameters
rho = 1.21; #approximate density at height range 50-100m
CLmax = 1.75
AR = 8.3
b = 2.82 # (m)
S = b**2/AR # (m^2)
W = 8.8 # (kg)

n_pos = 3 # Positive limit load factor
n_neg = -1 # Negative limit load factor

V_c = np.sqrt((2*W*n_pos)/(rho*S*CLmax)) # Cornering velocity (ms)
V_b = np.sqrt((2*W*-n_neg)/(rho*S*CLmax))
V_d = 22.5 # Maximum structural limit velocity (m/s)

V_s = np.sqrt((2*W)/(rho*S*CLmax))
print("V stall = ",V_s) # Stall speed (m/s)

# Define range of velocities
V_range = np.linspace(0, V_d, 100)
Vc_range= np.linspace(0, V_c, 100)
Vb_range= np.linspace(0, V_b, 100)

nc = (0.5*rho*S*CLmax*Vc_range**2)/W
nb = -(0.5*rho*S*CLmax*Vb_range**2)/W

# Create V-n diagram plot
plt.figure()
plt.axhline(y=n_pos, color='r', linestyle='--', label='Positive Limit')
plt.axhline(y=n_neg, color='b', linestyle='--', label='Negative Limit')
plt.axvline(x=V_c, color='g', linestyle='--', label='Cornering Velocity')
plt.axvline(x=V_s, color='m', linestyle='--', label='Stall Speed')
plt.axvline(x=V_d, color='c', linestyle='--', label='Max Structural Limit')

plt.plot(Vc_range,nc,'k')
plt.plot(np.linspace(V_c, V_d, 100),[n_pos for i in range(100)],'k')
plt.plot([V_d for i in range(100)],np.linspace(n_neg, n_pos, 100),'k')
plt.plot(np.linspace(V_b, V_d, 100),[n_neg for i in range(100)],'k')
plt.plot(Vb_range,nb,'k')

plt.xlim((-5, 30))
plt.ylim((-2, 4))

plt.xlabel('Velocity (m/s)')
plt.ylabel('Load Factor (n)')
plt.title('V-n Diagram')
plt.legend(loc='center right')
plt.grid(True)
plt.show()
```

# Bibliography

- [1] Blue Shark F250 4hrs Long Endurance 2500mm Wingspan Electric VTOL UAV
- [2] The E384 Mapping Drone
- [3] Baykar Bayraktar Mini UAV
- [4] Raven B RQ-11
- [5] Skywalker X5 Pro
- [6] ALBATROSS
- [7] JOUAV CW-007
- [8] Blue Shark F320
- [9] JOUAV CW-015
- [10] Mini Shark UAS
- [11] DT26M
- [12] The Tempest
- [13] Puma LE
- [14] Rolta Mini UAV
- [15] Workswell Wiris Enterprise - Integrated Thermal and Optical Sensor
- [16] Prana PM2.5 - Air Quality Monitor
- [17] LiPo Battery
- [18] Aircraft Performance - Climbing Flight
- [19] Aircraft Design: A Conceptual Approach - Daniel P Raymer
- [20] A procedure for Power consumption estimation of multi-rotor Unmanned Aerial Vehicle
- [21] Power required conversion to battery charge
- [22] Gimbal for optical stabilization
- [23] Deciding the geometric and aerodynamics parameters for UAV
- [24] First Weight Estimate Calculation Code
- [25] Estimation of Lift and Drag Characteristics of UTM Elang-1 UAV
- [26] T-MOTOR AT7215
- [27] TF16\*8 Propellers
- [28] Aircraft design: A Systems Engineering Approach - Mohammad H. Sadraey
- [29] Aerodynamics of Finite Wings